Scanning Microscopy

Volume 10 | Number 3 Article 13

8-22-1996

Applications of Laser Microprobe Mass Spectrometry in Biology and Medicine

Annette Bakker
University of Antwerp

Luc Van Vaeck
University of Antwerp

Wim Jacob
University of Antwerp, jacob@uia.ua.ac.be

Scanning Microscopy, Vol. 10, No. 3, 1996 (Pages 753-775) 0891-7035/96$5.00+.25
Scanning Microscopy International, Chicago (AMF O'Hare), IL 60666 USA

APPLICATIONS OF LASER MICROPROBE MASS SPECTROMETRY IN BIOLOGY AND MEDICINE

Annette Bakker[1], Luc Van Vaeck[2] and Wim Jacob[1]*

Departments of [1]Medicine and [2]Chemistry, University of Antwerp (UIA),
Universiteitsplein 1, B-2610 Wilrijk, Belgium

(Received for publication October 16, 1995, and in revised form August 22, 1996)

Abstract

Laser microprobe mass spectrometry (LMMS) provides spot analysis with a lateral resolution of 1-5 μm. Focused laser ionisation, combined with mass spectrometry, yields information on elements, molecular identification of inorganic substances, and structural characterisation of organic molecules of typically less than 2-3 kDa. Quantification in complex heterogeneous systems, such as biological materials, is not possible at the present state of the art. The strength of the method lies in the qualitative information on the molecular composition of the analyte, not just element detection, with a lateral resolution at the light microscopy level. The applications of this technique in the field of biomedicine and biology are illustrated by examples that demonstrate the use of this qualitative information in practical test cases.

Key Words: Laser microprobe mass spectrometry, time-of-flight, Fourier transform, microscopy, analysis, calcium.

*Address for correspondence:
Wim Jacob
Department of Medicine,
University of Antwerp (UIA),
Universiteitsplein 1,
B-2610 Wilrijk, Belgium
Telephone number: +(32) 3 8202509
FAX number: +(32) 3 8202603
E.mail: jacob@uia.ua.ac.be

Introduction

Fundamental progress in structural biology and biomedicine is based on the morphological differentiation of species, tissues, cell structures and substructures on the one hand and specification of the chemical constituents and interactions involved on the other hand. The instruments and methods employed inherently reflect this duality (Table 1). Initially, light microscopy, and later on, electron microscopy, provided the essential tools for observation on the cellular to subcellular level. For a long time, these methods have been combined with cytochemistry, employing specific chemical reactions to visualize elements or enzymatic reactions. However, the accuracy of the chemical information depends on the specificity of the interaction between the reagent and the components aimed at. This is not always obvious. As a result, chemists have been elaborating methods for direct microanalysis of tissue samples.

Analytical electron microscopy (AEM) and the related electron energy loss spectroscopy (EELS) are widely used in biology and biomedicine. Proton-induced X-ray emission (PIXE) or nuclear methods provide better detection limits, but lateral resolution remains in the light microscopy range. The interaction of electrons or protons in these so-called non-destructive methods occurs at the level of the analyte atoms. However, there is a need for direct information on the inorganic or organic molecules as such, not just on the elements present or on cytochemical reaction products.

Identification of the analyte molecules can be achieved by local ionisation of the sample and subsequent mass spectrometric analysis of the emitted ions. Secondary ion mass spectrometry (SIMS) uses a primary ion beam to ionise the sample locally; laser microprobe mass spectrometry (LMMS) employs a focused laser. In both cases, the morphological information is restricted to the μm-range. LMMS has been especially proven to allow direct determination of the molecular composition of both organic and inorganic compounds. Additionally, numerous structural ions are generated for detailed identification.

Table 1. Survey of currently used techniques for morphological and chemical analysis of biomedical samples.

Technique + interactions	lateral resolution	chemical information
Light microscopy based: light in, light out	μm level	* elemental: cytochemistry or staining * organic molecules: labelling
Electron microscopy based electrons in, electrons out	approximately 1 nm	**classical EM**: * elemental: electron density * organic molecules: labelling or cytochemistry **analytical EM**: * elemental: X ray, quantitative (all with Z > 11) **EELS**: * elemental: energy loss, quantitative (all with Z > 4)
Nuclear microscopy Mev protons in, X-ray out	μm level	*elements: mapping, quantitative, all Z > 15
Mass spectrometry based SIMS: ions in, ions out LMMS: photons in, ions out	μm level	**SIMS**: * elemental: indirect speciation, qualitative **LMMS: TOF and FT**: * elemental: high mass resolution and accuracy * direct speciation and organic molecule identification

The use of LMMS in biological and biomedical analysis still is at an experimental stage. The purpose of this paper is to describe the method and to survey how LMMS fills the gap left by the other microanalytical techniques. Examples from our laboratory will show how LMMS can be used in practice, for instance, to verify the cytochemistry, to complement the AEM element analysis with molecular information, and to characterize organic molecules by structural ions. In this way, we will outline the possibilities as well as the limitations of LMMS for bio-applications so that the researchers in the field can assess whether or not LMMS may provide answers to their particular questions.

LMMS: Instrumentation and Methodology

Pulses from an ultraviolet (UV) laser focused to a 1 to 5 μm spot ionise the region of interest in the sample (Van Vaeck *et al.*, 1993a,b). The ions are subsequently separated according to their mass-over-charge ratio (m/z). The elemental composition of the detected species can be derived from the m/z. Combination of these data allows identification of the analyte. In principle, quantification is possible since the signal intensity reflects the number of ions and hence the concentration in the sample. Specimens can be conducting or dielectrical, thick or 0.25 μm thin, so that current preparation methods for microscopy and microanalysis are adequate. Depending on the power density during laser irradiation, molecular or elemental information is obtained. The development of LMMS goes back to the 1970's (Hillenkamp *et al.*, 1975). The first generation of commercial LMMS employed a time-of-flight (TOF) mass spectrometer (MS) (Vogt *et al.*, 1981; Dingle *et al.*, 1981). The mass resolution was found insufficient (Van Vaeck *et al.*, 1993a). Therefore, recent developments involve the use of a Fourier transform (FT) mass analyzer (Van Vaeck *et al.*, 1994a). The high mass resolution of FT LMMS increases the specificity of the method significantly.

Time-of-flight (TOF) LMMS

The commercial instruments share most of the essential features but differ with respect to the irradiation geometry, sample mounting and optics. Figure 1 shows the diagram of the LIMA 2A (initially Cambridge Mass Spectrometry, later on Kratos, Manchester, UK) (Dingle *et al.*, 1981; Ruckman *et al.*, 1984; Southon *et al.*, 1984). The ionising UV-laser is aligned co-linearly with the He-Ne laser, projecting a visible spot on the sample. Micromanipulators allow us to position the region of interest under microscopical observation. An ingenious combination of optical and mechanical devices permit analysis in transmission or reflection. In the transmission mode, the laser impinges on the sample side opposite to the one facing the mass spectrometer. Thin samples, up to 1 μm, can be analyzed. Reflection means that the laser is directed on the sample side from which the ions are extracted. Now, bulk specimens are also adequate. The lateral resolution is typically 1-3 μm (Dingle *et al.*, 1982).

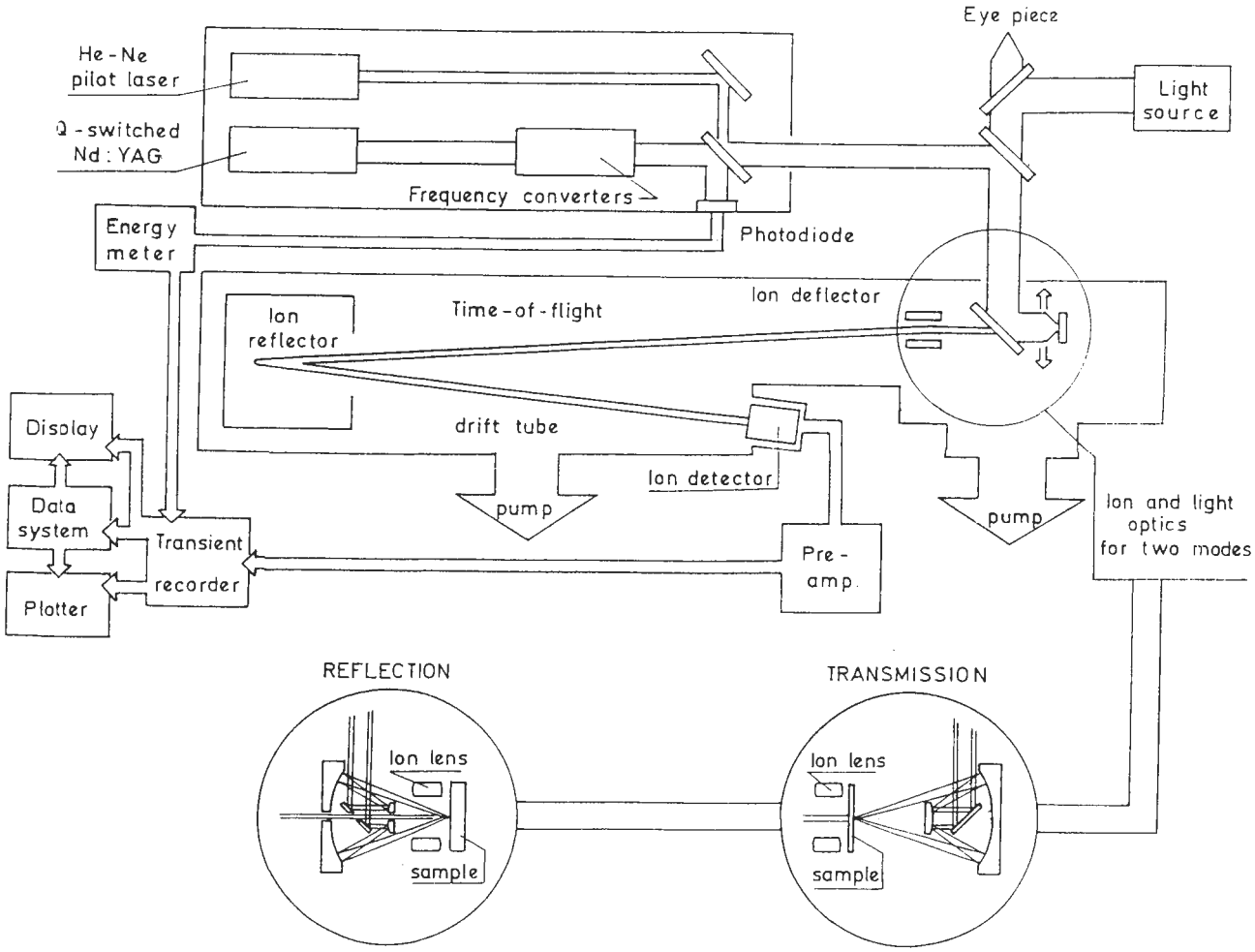

Figure 1. Schematic diagram of the Lima 2A laser microprobe mass spectrometer with time-of-flight mass analyzer (with permission of Van Vaeck *et al.*, 1994a).

The LAMMA 500 (Leybold-Heraeus, Köln, Germany, now SPECS, Berlin, Germany) irradiates the sample only in transmission (Vogt *et al.*, 1981). The lateral resolution is ultimately 0.5 μm, i.e., the diffraction-limited spot at 266 nm (Wechsung *et al.*, 1978; Guest, 1984). The spot size determines the sample volume analyzed and hence the detection limit. A spot of 1-2 μm is more routinely used. The mass resolution attains 850 for elemental ions at m/z 208 (Kaufmann *et al.*, 1979) and 500 for organic ions (Van Vaeck *et al.*, 1985). Detection limits go down to the 1 ppm-range for elemental ions (Kaufmann *et al.*, 1979; Guest, 1984; Verbueken *et al.*, 1988).

The LAMMA 1000 operates in reflection mode (Heinen *et al.*, 1983). Spot sizes are from 1-3 μm upwards (Hillenkamp *et al.*, 1982). For organic molecules, detection of organic complexes from a layer of less than 100 nm over a spot of 10 μm has been reported, corresponding to about 4 x 10^9 molecules (Holm and Holtkamp, 1989).

Improvements of the commercial instruments on a laboratory scale involve UV-illumination for better sample observation (Kaufmann, 1982), tunable dye-lasers for resonant ionisation (Muller *et al.*, 1985a,b; Verdun *et al.*, 1987) and post-ionisation to improve detection limits, reproducibility and differentiation between organic and inorganic ions (Schueler and Odom, 1987; Odom and Schueler, 1990). A thorough development was achieved with the so-called LAMMA 2000 (Kaufmann and Spengler, 1992a,b). The new optical design, based on a confocal UV-scanning microscope, improved sample observation. The ionising laser is directed along the normal on the sample and allows a diffraction limited lateral resolution of 0.5 μm routinely. A piezo-driven specimen holder permits analytical mapping. The mass spectrometer is improved for high-mass detection and offers a mass resolution up to 4500.

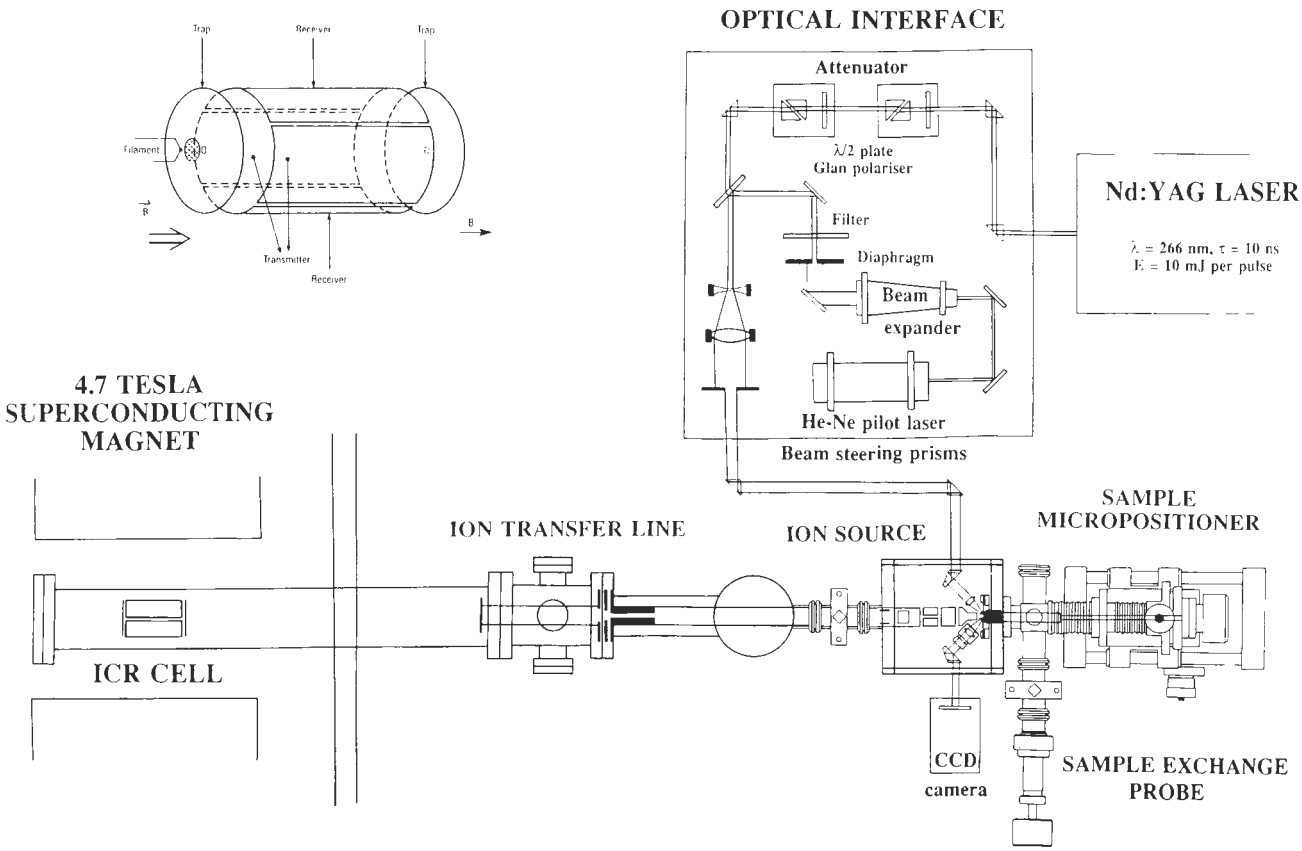

Figure 2. Schematic diagram of the Microfocus® Fourier transform laser mass spectrometer with external ion source. The insert shows the cylindrical FT MS cell (with permission of Struyf *et al.*, 1993).

Focused laser ionisation

All LMMS instruments perform ionisation at 266 nm under similar conditions (Van Vaeck *et al.*, 1994a). Energies from a few nJ onwards in a pulse of 4-15 ns yield power densities on the sample above 10^6 W·cm^{-2}. The laser impact leads to several desorption-ionisation (DI) processes, such as ablation, atomization, ultra-fast heating and evaporation of large organic molecules, direct ion emission from the solid or ion formation through ion-molecule interactions in the selvedge, i.e., the micro-cloud above the sample. Depending on the conditions, elemental ions, inorganic clusters, organic molecules, and fragment ions are generated. Up to now, little is really known about the DI in LMMS (Van Vaeck *et al.*, 1994a).

This explains the difficulties in quantitative LMMS. The ion yield is governed by the energy deposition in the analyzed micro-volume. The local energy regime is in turn a function not only of the UV-absorption of the analyte and the surrounding matrix, but also depends on optical properties such as refractivity or reflectivity. These parameters are impossible to control locally in an heterogeneous biological sample. As a result, the straightforward quantification using the local thermal equilibrium approach is not feasible (Mauney, 1985; Kaufmann, 1982). Moreover, the preparation of suitable standards is all but trivial (Verbueken *et al.*, 1988; Eeckhaoudt *et al.*, 1994; Van Vaeck *et al.*, 1994a). However, signal intensities recorded under the same instrumental conditions can be used to assess the local concentration.

In practice, spectra can be extremely complex due to the signals from the various constituents within the micro-volume. Deducing the sample composition is hindered by the lack of insight in the DI processes. High mass resolution becomes mandatory to separate the isobaric contributions to the detected signals and to determine unambiguously the elemental composition of the ions.

Mass analysis in TOF LMMS

The m/z-separation is based on the velocity difference imposed to ions of different m/z upon acceleration by an electrical field. The light ions having the largest speed cover a given trajectory in a field-free region faster than the heavier ions. As a result, time-separation occurs. The sequential arrival of ions is then recorded

and the time scale is calibrated into m/z using reference compounds. Mass resolution is improved by an ion reflector (Mamyrin *et al.*, 1973). The repulsing field slows down and reverses the direction of the ions. Ions with a kinetic energy above the mean value penetrate deeper in the reflecting field, and hence spend more time on a longer trajectory than the ions with less than average kinetic energy so that the flight time difference is compensated. In this way, the peak width is reduced and no sensitivity is lost.

TOF LMMS provides major advantages such as a rather inexpensive construction, simplicity of operation, speed of analysis, "ultimate" sensitivity by high transmission, inherent availability of full mass spectra and an unlimited m/z range. A disadvantage is the low mass resolution. Only nominal m/z values can be separated up to m/z 500. Furthermore, the separating power strongly depends on the ionisation kinetics. Ion formation in LMMS can be "prompt", i.e., during the 4-15 ns of the laser pulse, or continue over a few μs, i.e., "post-laser" DI. An essential requirement for the m/z-separation is that all ions enter the drift tube practically at the same time. Only the prompt fraction of the laser DI meets this requirement.

Fourier-Transform (FT) LMMS

Fourier-Transform mass spectrometry (MS) analyzers are reputed to provide routinely a mass resolution of over 100,000 and a mass accuracy within the ppm-range (Holliman *et al.*, 1994). The first attempt to construct an FT LMMS was started at the University of Metz (Pelletier *et al.*, 1988). The laser impinges perpendicularly on the sample. The theoretical spot is 3-4 μm, but crater sizes of 6-10 μm are typically used. Post-ionisation by a second laser is possible. Mass resolutions over 100,000 were reported for elemental ions, and mass accuracy is better than 10 ppm. A detection limit of 1 ng was found for atrazine in the single shot mode (Krier *et al.*, 1994). Later on, two different setups were built at the IBM laboratories (Brenna *et al.*, 1988; Ghaderi, 1988). The laser irradiates the sample under 45°. The spot size is about 9 μm and the mass resolution 400,000 for Pb^+-ions. The resolution of the observation optics is 5-8 μm (Brenna and Creasy, 1988; Brenna, 1989, 1991). A similar instrument is commercialised by Finnigan FTMS (Madison, WI). An instrument with external ion source was converted into an FT LMMS at the University of Antwerp (Van Vaeck *et al.*, 1993b). Figure 2 shows the schematic diagram. The laser hits the sample under 45°. The lateral resolution is routinely better than 5 μm. The mass resolution attains typically 4 x 10^6 for 56 Fe^+, 2 x 10^6 for Au^+, while for organic ions 3 x 10^5 is normally reached at m/z 300 and 1 x 10^5 at m/z 1000. Mass accuracy is better than 1 ppm. Detection limits are at 10^8-10^9 atoms evaporated for elemental ions or 300 fg (femtogram) for organic ions (Struyf *et al.*, 1994; Van Roy *et al.*, 1994). The sample is observed with a 700X magnification, providing a 1 μm resolution. The set up is now marketed as MicroFocus® by Bruker Instruments, Inc. (Billerica, MA).

Fourier-Transform mass spectrometers in LMMS

The m/z separation is achieved in a small cubic or cylindrical cell (insert in Fig. 2) in a magnetic field B of typically 3-5 Tesla (Marshall and Verdun, 1990). A low DC voltage (e.g., 1 V for positive ions) on the two trapping plates force the ions on a forth-and-back trajectory in the potential valley. Due to the Lorentz force, ions also orbit in a plane perpendicular to B with a frequency, inversely proportional to their m/z. A radio-frequency excitation field, applied to the transmitter plates with the ion's frequency, increases the initially small orbit radius so that the ions move close to the receiver plates and induce image currents. The excitation field also converts the initial random phase of different ions with the same m/z into a coherent movement. The detected signal is a sine wave with a frequency, corresponding to the m/z of the ions and an amplitude, reflecting the number of ions in that packet. The signal takes the form of a damped wave because the coherence is lost with time by space charge effects and collisions with the residual molecules in the cell. The decay time of the signal directly determines the resolution of the mass spectrometric signal. The length of the transient is optimised by, for instance, the cell plate voltages, not by cutting the ion beam as in magnetic mass spectrometry. In fact, best sensitivity is reached at high mass resolution in FTMS, as opposed to all other mass spectrometers.

The m/z typically ranges from m/z 20 to 15,000 as a result of the magnetic field strength and the bandwidth of the electronics. As an ion trap, FTMS requires ionisation pulses, which can continue for milliseconds. Hence, prompt and post-laser generated ions can be integrated. Panoramic registration is performed at relatively low mass resolution, primarily because of the detection electronics. Operating costs are substantial by the superconducting magnet while the optimisation of the instrument settings is more critical than in, for instance, TOF MS.

A mass spectrum is always related to the initially produced ion bunch by the characteristics of the mass analyzer itself with respect to the transmission as a function of kinetic energy and initial emission angle, formation period of detectable ions, etc. As a result, mass spectra from TOF and FT LMMS may look quite different (Van Vaeck *et al.*, 1994a). Specifically, FT LMMS

integrates the prompt and post-laser generated ions while TOF LMMS only detects the prompt ions. TOF LMMS can deal with broad kinetic energy distributions up to 15 eV (Hillenkamp *et al.*, 1975; Mauney and Adams, 1984; Michiels *et al.*, 1984; Housden *et al.*, 1989;); FT LMMS only with a range of 1 eV. As a result, the question arises as to what extent the detected signals in FT LMMS provide a better basis for analyte identification, apart from the higher mass resolution and mass accuracy.

Survey of morphological and chemical analysis methods

Light microscopy is still one of the most useful techniques for diagnostic applications. It is cheap, simple and capable to handle a large number of samples, but lateral resolution remains in the 1 μm-range unless special techniques are used. For morphological analysis, cytochemical techniques can be applied to show the subcellular information. Staining or labelling techniques must be used to make the presence of elements detectable. Organic molecules can only be detected indirectly by the use of immunocytochemical techniques. The preparation of biological sections becomes a key step. The morphological information must be kept intact and the original localisation of given components at specific sites or in compartments of the biological matrix must be preserved. Obviously, unwanted chemical interactions must be avoided as well.

Responding to the desire for better lateral resolution and increased chemical specificity, electron microscopy (EM) methods have gained wide acceptance (Glauert, 1974). The classical EM for morphological applications relies again on the specificity of the cytochemical reaction. Since the visibility of elements in EM demands a high electron density, only elements with a high atomic number (Z) can be localised. To visualize organic molecules, labelling with electron dense elements is usually necessary. Note that the electron dense elements are traced, not yet identified. In order to identify the traced elements, EM is combined with X-ray spectrometry. Current instruments with X-ray analysis do not provide optimal sensitivity, and dedicated microprobes sacrifice some of the lateral resolution (Reimer, 1989). However, both types are now denoted as AEM. Additionally, the element-specific energy loss of the impinging electrons is resolved and quantified in EELS (Egerton, 1986). The prime asset of EM based methods is their unsurpassed lateral resolution while cytochemical reactions are no longer a prerequisite. In the flood beam mode, EELS offers even better lateral resolution, but sensitivity remains a matter of debate. X-ray based detection offers the easy quantification (Lorimer, 1984). Speciation of inorganic compounds, i.e., determination of the molecular composition, must be based on the relative element ratios. This approach is highly questionable when complex mixtures such as biological materials are involved. Organic compounds cannot be characterized directly unless cytochemistry is applied.

The recently emerging "nuclear microscopy" actually denotes a range of methods (Malmqvist, 1986; Watt and Grime, 1988; Watt *et al.*, 1990; Szokefalvi-Nagy, 1994). Application of nuclear microscopy in biology and medicine is recently surveyed (Bara *et al.*, 1996). The technique provides high elemental sensitivity as a result of the MeV proton beam that bombards the sample to generate the detected X-rays. Analytical mapping is available with a lateral resolution of 1-3 μm (Grime *et al.*, 1991; Forslind and Emilson, 1992; Edelman, 1994). Sample observation with a resolution in the 0.5 μm range is based on the secondary ion emission. Emitted ions improve the observation (Bench and Legge, 1989).

SIMS (Burns-Belhorn and File, 1979; Benninghoven *et al.*, 1987) employs keV ions to interact with the sample and mass analysis of the elemental ions and the small cluster ions generated. Fingerprinting is used for speciation. As a mass spectrometer it provides full periodic table coverage including the light elements and isotopic information. SIMS can be used to generate mass selected images of the sampled area. The diameter of the impinging beam ranges from 0.1 to 1 μm and a total area of up to, e.g., 250 μm can be rastered. Quantification requires appropriate standards. Applications of SIMS in medicine have been recently reviewed (Fragu *et al.*, 1994).

This discussion shows that LMMS fills in the gap left by the other analytical techniques (Eeckhaoudt *et al.*, 1994; Van Vaeck *et al.*, 1994a,b). The molecular composition of inorganic and organic constituents, especially, can be determined. Major drawbacks are the lateral resolution, the absence of quantitative capabilities and in most instruments, analytical mapping is not provided.

Applications

Several reviews cover the LMMS applications (Kaufmann, 1982; Verbueken *et al.*, 1985; Kaufmann *et al.*, 1989; Eeckhaoudt *et al.*, 1994). Therefore, in this paper, we restrict ourselves to selected experiments from our laboratory, using the LAMMA 500 TOF LMMS (Leybold-Heraeus, Köln, Germany) and the FT LMMS with an external source (Bruker Instruments Inc., Billerica, MA). The EM employed includes a JEOL 1200 EX-TEMSCAN (JEOL, Tokyo, Japan) with a scanning attachment for scanning transmission electron microscopy (STEM), coupled to a NORAN TN 5500 (Noran Instruments, Middleton, WI) energy dispersive

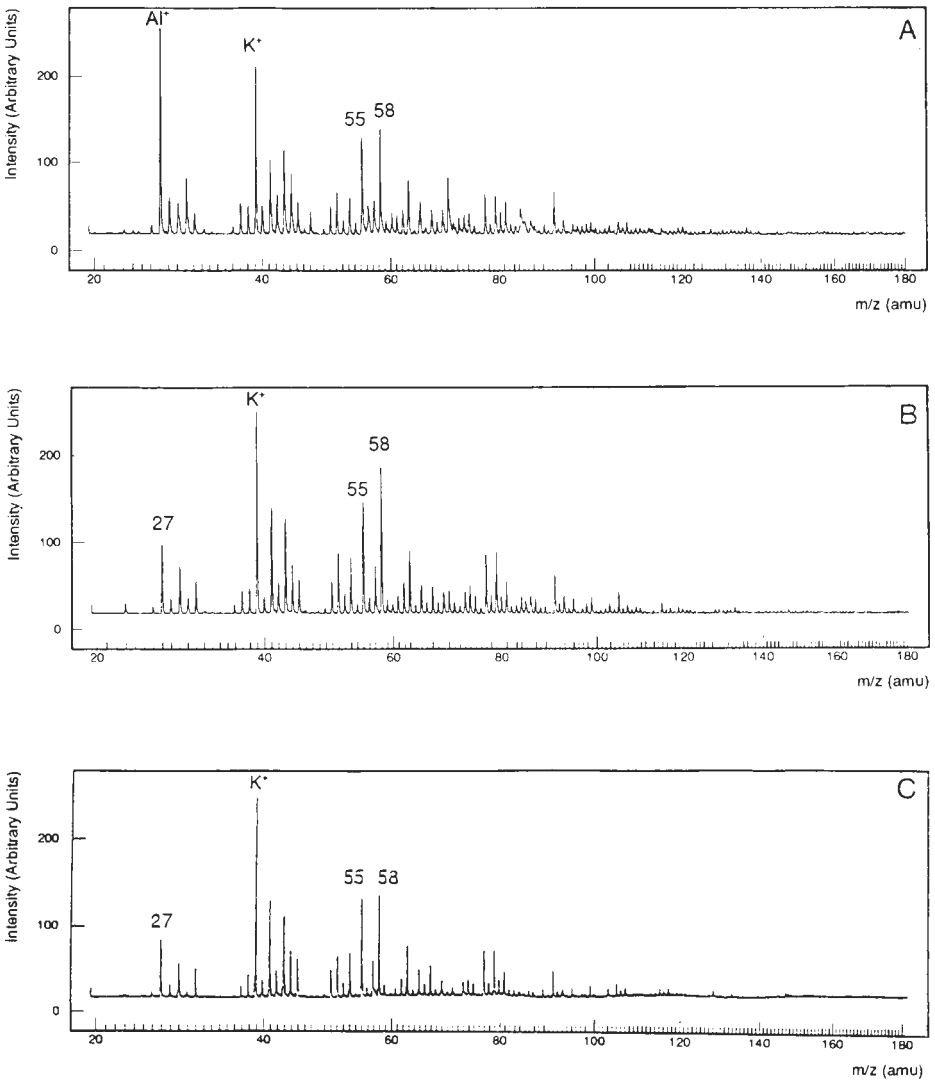

Figure 3. Positive ion mass spectra recorded by TOF LMMS for the analysis of the secondary lamellae of bullhead fish gills. (**A**) Positive ion mass spectrum of a secondary lamella edge in gill tissue of an aluminum-exposed fish; (**B**) averaged positive ion mass spectrum of a lamella from an unexposed bullhead; (**C**) positive ion mass spectrum from the embedding medium (with permission of Eeckhaoudt *et al.*, 1994).

X-ray (EDX) analysis system and an IBAS 2000 digital image computer (Kontron, München, Germany). PIXE data were collected on the Oxford proton scanning microscope (Grime *et al.*, 1991). For the sake of clarity, the examples are classified according to the level of information. First, element localisation is dealt with; then, applications involving structural information of inorganic molecules, i.e., speciation, and finally, the direct characterisation of organic molecules in the complex environment of a biological tissue is highlighted.

Element localisation

Localisation of aluminum in fish gills: Due to the acidification of poorly buffered environments, aluminum (Al) is set free from soils and transported to rivers and lakes. The increased Al content in acidified water revealed to be a significant cause for fish death. Fish gills are considered to be an important target for Al contamination because of their large exchange surface. Therefore, bullheads were subjected to acidified water with elevated levels of Al. The objective of the experiments was to localise Al in the gills in order to gain insight in the toxicity mechanism *in vivo*. The gills were cut in small pieces of approximately 1 mm^3, fixed in a phosphate buffered (0.1 M, pH 7.4) 2.5% glutaraldehyde solution, dehydrated and imbedded in epoxy-resin. Due to the pH, there is hardly a loss of Al. Several samples were subjected to a comparative analysis by LMMS, EM and PIXE.

Figure 3 illustrates the positive mass spectra recorded by TOF LMMS for the analysis of the secondary lamellae of the bullhead (Eeckhaoudt, 1994; Eeckhaoudt *et al.*, 1994). Spectrum (**A**) and (**B**) originate from the edge of the lamellae from an exposed and an unexposed bullhead respectively. Spectrum (**C**) is recorded from the embedding medium. The perforation diameter of the section upon laser impact is typically 1-2 μm. The base peak in the spectrum from the exposed fish is due to the aluminum ions at m/z 27 while the Al^+ ions only yield

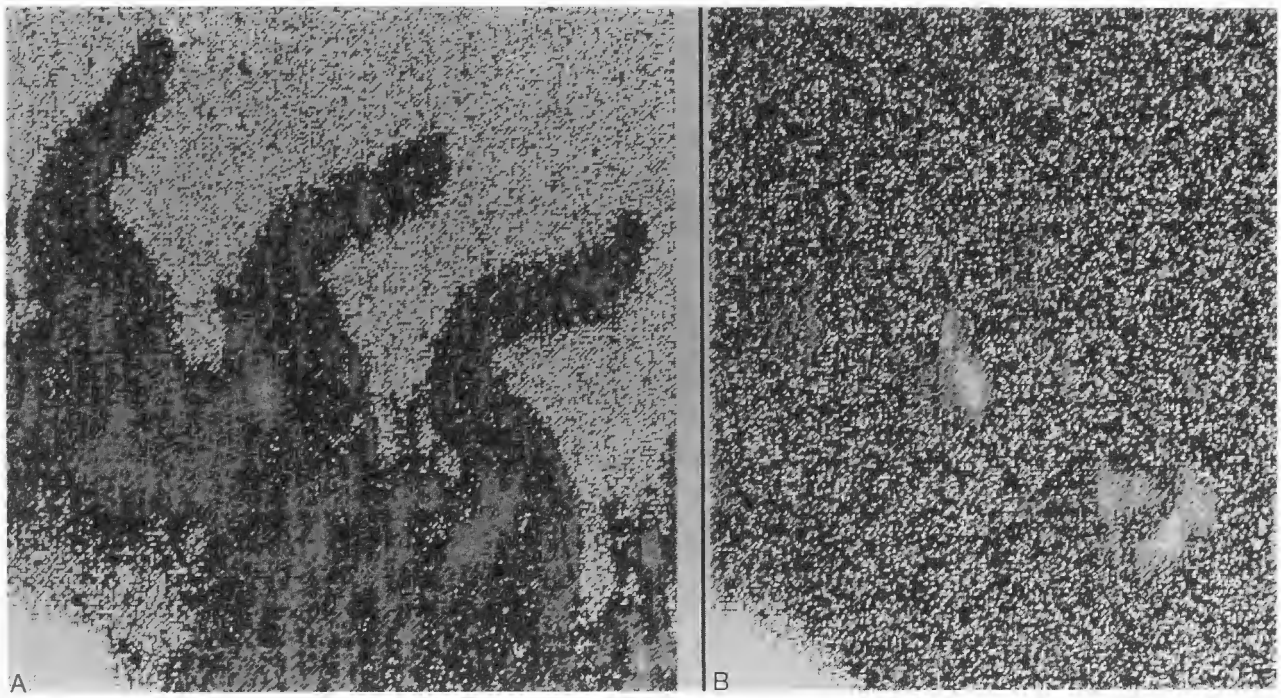

Figure 4. Phosphorus and aluminum maps of a 250 m 250 m scanned area of aluminum-exposed bullhead gills. (**A**) The contours of the secondary lamellae can be followed in the phosphorus map; (**B**) the locations of high aluminum distribution are indicated by bright spots (with permission from Eeckhaoudt *et al.*, 1994).

---

a minor signal in the spectra from the control and the embedding polymer. Apart from the prominent K^+ ions, major peaks are found at m/z 55 and 58. These signals are assigned to $C_4H_7^+$ and $C_3H_6O^+$., i.e., structural ions from the epoxy resin. This already indicates the potential of LMMS to combine element localisation with real organic analysis. Peak intensities still allow a qualitative assessment of the concentration levels in the tissue. The accumulation of Al^+ occurs on very few spots along the edge of the lamella. Our TOF LMMS performs spot analysis and no mapping while the image through the observation microscope is rather poor. As a result, the method becomes laborious whenever elements have a scattered distribution, because hundreds of spectra have to be recorded "manually" before the specific site of accumulation is hit.

PIXE was also applied to this problem. Figure 4 shows the element maps for phosphorus (P) (Fig. 4A) and Al (Fig. 4B) over a 250 μm x 250 μm area. The P-map serves to recognise the contours of the lamellae. The Al distribution image shows accumulation at the base of the secondary lamellae. Note that a higher resolution could be obtained by using a smaller raster area. For quantitative purposes, point spectra are recorded. Table 2 surveys the Al- and P-concentrations in selected spots, shown on the accompanying sketch (Fig. 5). Sites corresponding to the bright spots in Figure 4B show Al-levels in the 1% range, which is 10 to 100 times higher than the blank value of the embedding medium. These experiments demonstrate the practical advantages of the PIXE technique, namely, mapping, excellent detection limits, and easy quantification. The major drawback is the limited resolution for sample observation. The development of scanning transmission ion microscopy in nuclear microscopy aims at the achievement of a resolution for sample observation in the order of 50 nm (Bench and Legge, 1989). As to the lateral resolution up on analysis, current research focuses on a 100 nm probe (Breese *et al.*, 1992; Grime *et al.*, 1991). The technique needs expensive accelerator equipment.

As a result, AEM remained useful in this research. The mapping capabilities of STEM EDX were employed to monitor the Al distribution. The major asset was the higher lateral resolution compared to PIXE. Point spectra confirmed the occurrence of Al accumulations at the edges of the secondary lamellae and the enrichment sites could be visualised at the ultra-structural level. However, the sensitivity is appreciably lower than in LMMS and PIXE.

In conclusion, as to element localisation, the morphological information obtained with LMMS and PIXE

Table 2. Results from point spectra analyses, recorded in the region depicted in Figure 4. bdl = below detection limit. The locations of the spots analysed are indicated in Figure 5.

Location	Element Concentration Al (%)	P (%)
1. Base secondary lamella	1.2	0.87
2. Base secondary lamella	1.1	0.87
3. Base secondary lamella	0.35	0.28
4. Secondary lamella edge	0.22	0.41
5. Secondary lamella edge	0.05	0.08
6. Close to secondary lamella edge	0.02	0.02
7. Inside secondary lamella	0.03	0.26
8. Inside primary lamella	0.03	0.21
9. Embedding medium	0.10	bdl
10. Embedding medium	0.02	bdl

is inferior to that of EM, but sensitivity is better. LMMS is handicapped by the lack of mapping and quantification capabilities.

Calcium distribution in isolated rat hearts subjected to ischemia and reperfusion: Mitochondrial contact sites have been described as dynamic micro-environments, created by the fusion of the inner and outer mitochondrial membranes (Hackenbrock, 1968; Knoll and Brdiczka, 1983). The number of these sites can be quantified with morphometric techniques as the percentage of the mitochondrial membrane area occupied by contact sites (Baddeley *et al.*, 1986). Their number highly depends on the energy state of the cell (Jacob *et al.*, 1992). Contact sites are functionally considered as highly organised energy channels between the energy consumption sites in the cytosol and the energy production sites in the mitochondria (Biermans *et al.*, 1990; Bakker *et al.*, 1994a; Wallimann, 1994). The results from a previous study indicated that contact site-formation is a calcium sensitive phenomenon (Bakker *et al.*, 1993, 1994b). To investigate whether the quantification of the contact sites represents a calcium sensitive morphological tool, the morphometric EM data (Bakker, 1995; Bakker *et al.*, 1995a) were compared to concentration assessments by FT LMMS. Isolated rat hearts were subjected to short periods of ischemia with or without subsequent reperfusion. Ischemia is a complex process arising when the arterial flow in the tissue is interrupted. At the end of each experiment, the hearts were perfusion fixed and the tissues were processed following regular schemes. As a consequence, only fixed Ca could be detected.

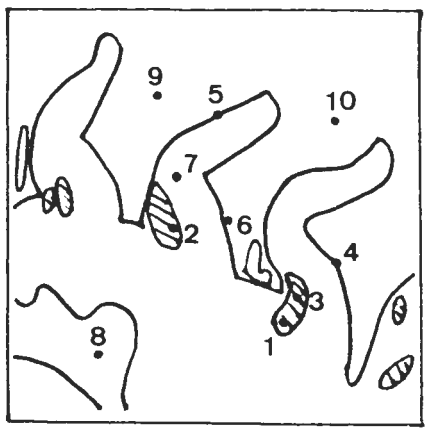

Figure 5. Sketch of the analysed lamella. The locations of the recorded point spectra of the section are indicated by numbers. The element concentrations for Al and P in selected spots are shown in Table 2 (with permission from Eeckhaoudt *et al.*, 1994).

Table 3. Functional and cellular effects of ischaemia and reperfusion on the isolated rat hearts. The calcium levels were estimated by FT LMMS. sem = standard error of mean.

ischaemia (minutes)	reperfusion (minutes)	Ca level[1] (FT LMMS)	% contact sites ± sem
-	-	+	35 ± 2
1	-	++	43 ± 2
2	-	+	37 ± 2
5	-	-	33 ± 1
10	-	--	31 ± 2
15	-	+	38 ± 1
20	-	++	30 ± 2
2	1	+++	40 ± 5
2	5	++	38 ± 1
2	15	+	34 ± 2
10	1	inhomog.	31 ± 5
10	5	+++	35 ± 1
15	5	++++	32 ± 5

[1]Ca level = semi-quantitative evaluation of the calcium content (by FT LMMS) by means of a scale normalised at + for the control preparation.

The results are summarised in Table 3. Up to 6 significant intensity levels were defined in FT LMMS to assess of the local calcium concentrations. Comparison of the calcium levels with the fractional contact site area

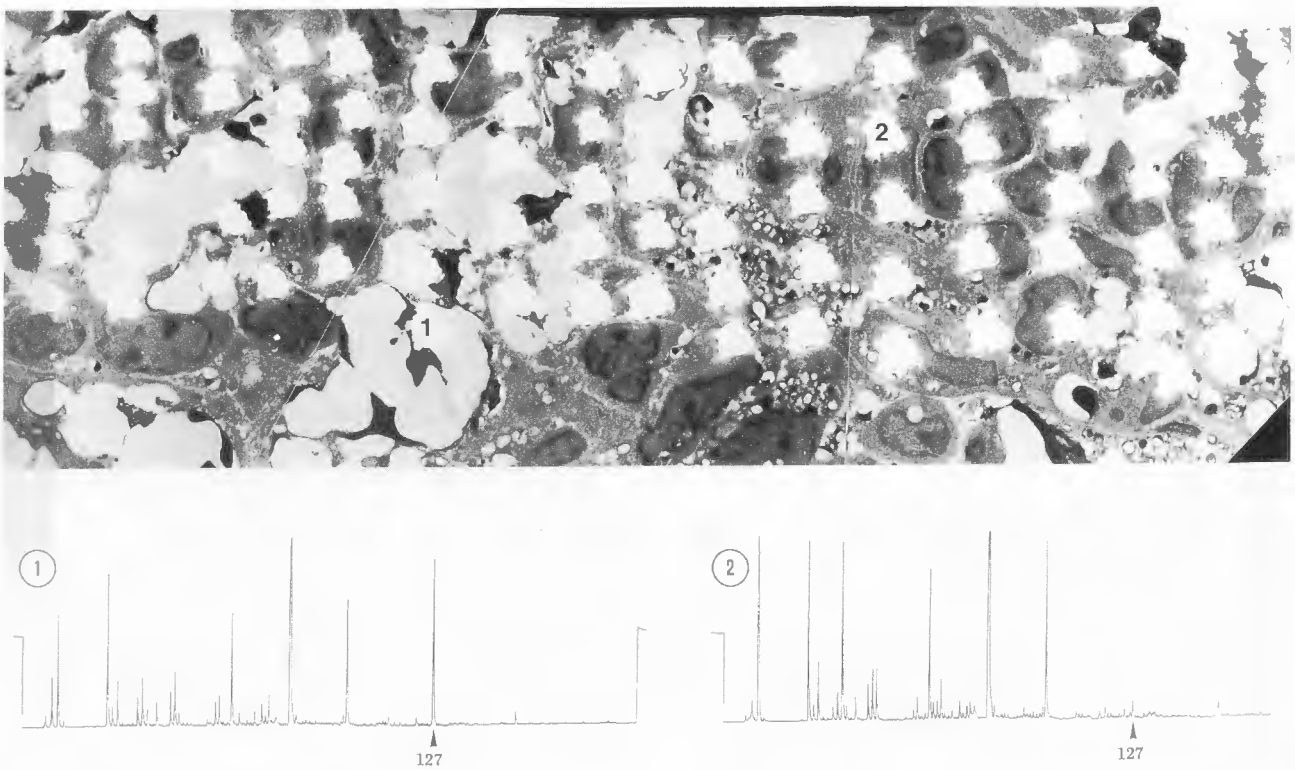

Figure 6. Negative ion mass spectra of a mesenteric lymph node from a dog subjected to amiodarone treatment. Since amiodarone is an anti-arrythmic drug containing iodine, the amiodarone can be localised by I-elemental ions which are detected with good sensitivity at m/z 127. (**1**) Analysis of a dense inclusion body containing amiodarone; (**2**) refers to a nucleus or a macrophage showing the virtual absence of a I-peak (with permission from De Nollin *et al*,. 1986).

---

derived from morphometric analysis shows both consistent as well as divergent trends. Specifically, up to 15 minutes of ischemia without reperfusion, the calcium level in FT LMMS roughly parallels the fractional contact site-area with a maximum after 1 minute. However, a strong discrepancy between the calcium level and morphometric data occurs after a 20 minute ischemic period. The fraction of contact sites still decreases while the calcium level rises. This could be associated with the occurrence of rigor contracture, whereby reperfusion does not lead to functional recovery. If subsequent reperfusion is applied, the morphometric data seem to correlate well with the calcium level when the ischemic period does not exceed 2 minutes. However, up on reperfusion after 10 minutes ischemic periods, complete disagreement between the two methods occurs. The number of contact sites tends to remain constant, while the calcium content becomes extremely high. The explanation of this phenomenon is not yet clear. These observations allowed to conclude that the quantification of contact sites does provide a good basis to assess the intracellular calcium content under quasi-physiological. In pathological situations, however, this correlation is lost. In spite of the limitations of LMMS as to quantification, comparative assessment of the local concentrations in consecutively analyzed samples is feasible. Proper precautions are needed to maintain sample thickness, focusing of the impinging laser and the many instrumental parameters. Summarising, the combination of EM with LMMS proves to be a matching set of techniques. It becomes possible to combine detailed morphological information with specific data on the chemical composition.

Localisation of a labelled drug by element information: A very interesting type of applications involves the localisation of administered drugs in the tissue. Although LMMS offers the potential for direct localisation of organic molecules, it must be realised that LMMS only detects organic ions from the analyte in the upper 10-50 nm of the section, even if the crater is much deeper (Van Vaeck *et al.*, 1988). Assuming that 100 ions on the detector are required for a significant peak and taking instrumental parameters into account, it turns out that the local concentration of the organic molecules must be 1-10% in the upper layer of the sample. This condition is only met in exceptional cases, unless local inclusions are formed.

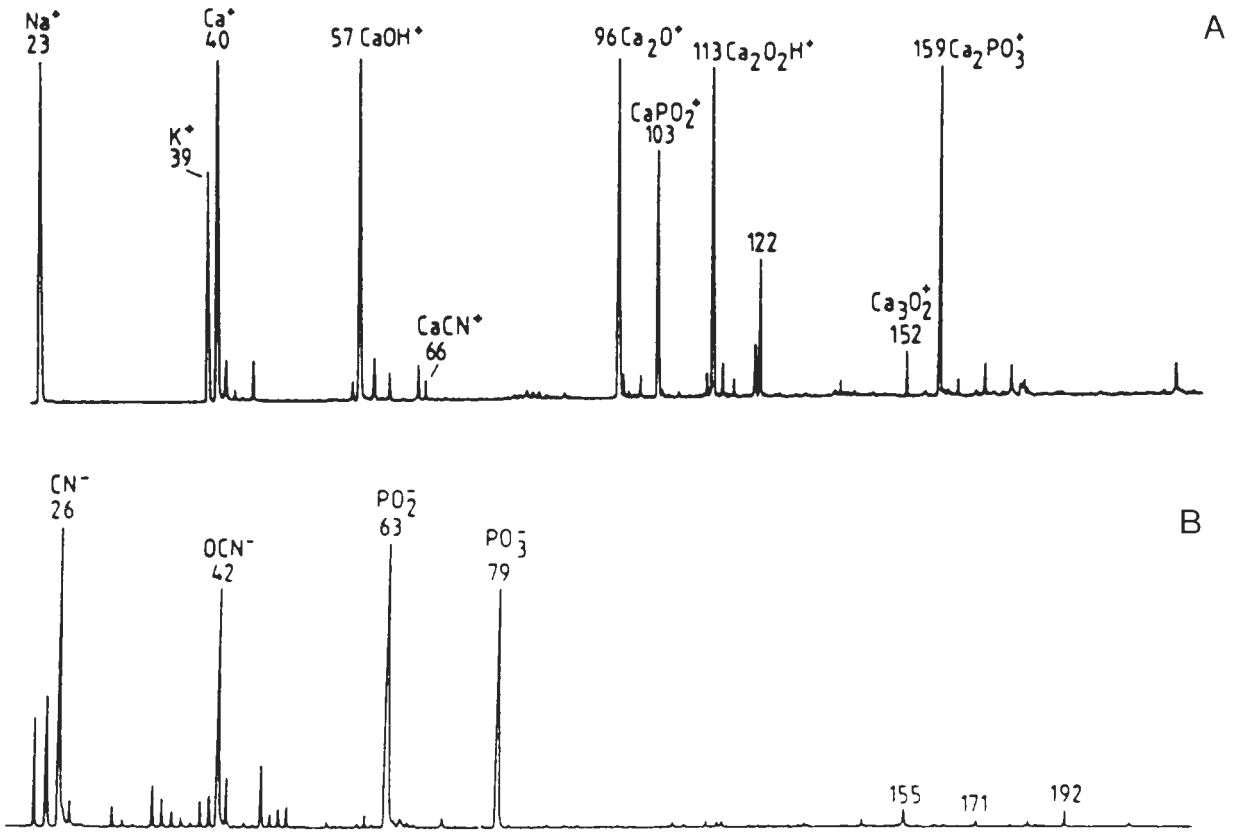

Figure 7. Typical mass spectra in the (**A**) positive and (**B**) negative ion detection mode recorded from a microlith, clearly showing that calcium-elemental ions are present as a calcium phosphate (with permission from Verbueken *et al.*, 1992).

One way to circumvent this problem consists of the use of drugs containing or labelled with a specific element. In that way, the analytical problem is reduced to element detection, for which better detection limits are reached. This was exploited in the study whereby dogs and rats were subjected to amiodarone treatment (De Nollin *et al.*, 1986). Amiodarone is an anti-arrythmic drug containing iodine. The I^- ions are detected with good sensitivity at m/z 127. Figure 6 shows the electron micrograph of a mesenteric lymph node section from an amiodarone treated dog after LMMS analysis. The poor observation capabilities of TOF LMMS explain the need to raster the entire sample. Each single shot produces a complete mass spectrum. The EM micrographs taken before analysis then serve to select the spectra as a function of the morphological structures. Two examples at positions 1 (dense inclusion body) and 2 (nucleus or macrophage) show the accumulation of amiodarone at given sites. The results were verified by an independent approach consisting of autoradiography at the light microscopical and on the EM level. Tritium labelled amiodarone was administered. These results confirmed the localisation by LMMS. Additionally, at the ultrastructural level, the labelled compound proved to be associated with lysosomal structures in the macrophages.

Calcium distribution in lidocain-perfused rat heart: Calcium ions are essential in the excitation-contraction coupling. Depriving the heart of its normal extracellular calcium causes an electro-mechanical dissociation. Subsequent re-introduction of calcium does not result in a restoration of its function, but results in massive tissue disruption, the release of enzymes and severe contracture of the muscle. Zimmerman and Hülsman (1966) called this phenomenon the calcium paradox. Although there is not yet consensus about the exact mechanism, it is clear that the calcium paradox is accomplished by a massive calcium accumulation. One of the hypotheses is that during calcium depletion, sodium enters the cell. During the calcium repletion, the accumulated sodium is exchanged for calcium. To investigate the possible role of sodium, the effect of lidocaine treatment on the extent of the calcium paradox was investigated by TOF LMMS (Bakker *et al.*, 1995b). Lidocaine is a class IB anti-arrythmic drug which is known to

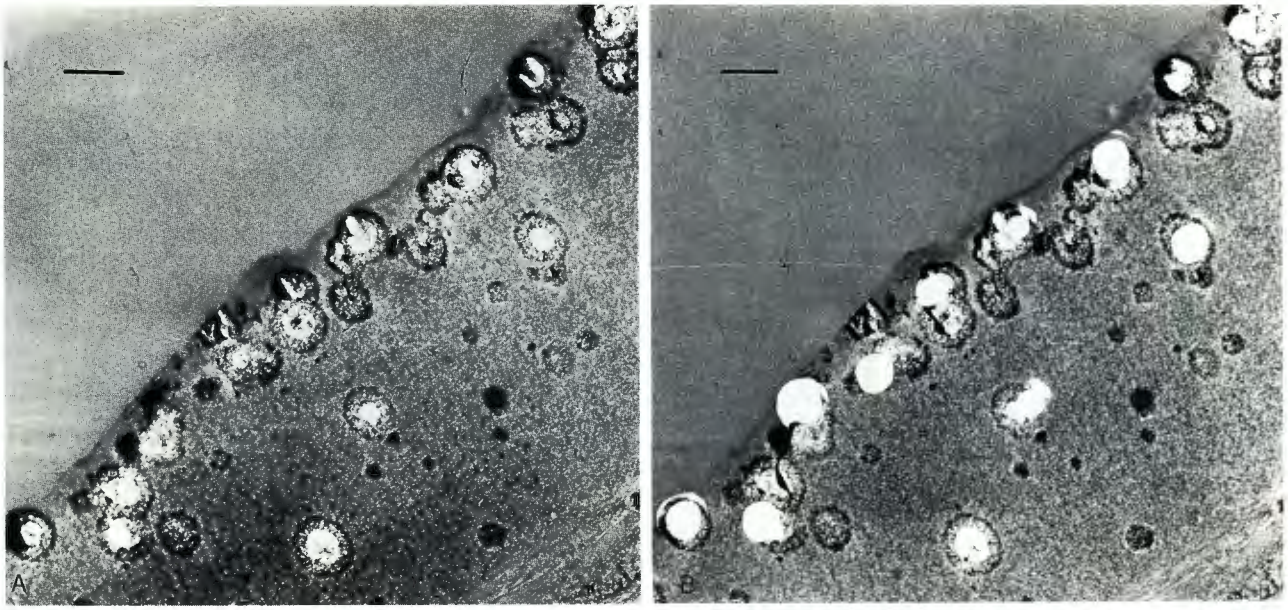

Figure 8. Transmission electron micrographs of Bowman's membrane of a patient (**A**) before and (**B**) after analysis with TOF-LMMS. Bar = 2 μm (with permission from Vandeputte *et al.*, 1989).

block the fast inward current of sodium. For this study, the free Ca^{2+} was precipitated by oxalate followed by pyroantimonate (Jacob *et al.*, 1984). After embedding, sections of 250 nm were prepared on Cu-Rh finder grids. Because of the poor visibility in the TOF LMMS microscope, complementing low magnification electron micrographs were made before and after analysis. Five groups of samples were compared. The control hearts were perfused with a modified Krebs-Henseleit buffer for 30 minutes. Ca-depletion was achieved by a ten minute perfusion with a similar buffer, not containing Ca. Ca repletion was performed by a subsequent perfusion with a Ca containing buffer for 10 minutes. Lidocaine treatment was achieved by addition of 0.1 mM lidocaine to the perfusion buffers.

The TOF LMMS assessment of the local Ca levels was performed by consecutive analysis of the different samples under the same conditions, without standards. The absolute intensities of the Ca^{+} signal at m/z 40 were measured. The average calcium levels determined up on depletion and repletion are essentially identical for the lidocaine treated and untreated heart tissues. Therefore, we suggested that 0.1 mM lidocaine may not be able to prevent the calcium accumulation accompanying the calcium paradox in rat hearts.

The application of LMMS in this study was motivated by its better sensitivity in comparison to our AEM. In conclusion, LMMS proved to be useful as an element specific technique to obtain in a fairly short period valuable estimates on relative concentrations. Considering the relative standard deviations, the concentration differences must be at least a factor 2. Otherwise stated, LMMS may become inadequate to study the pharmacokinetics in detail. However, due to the poor resolution available from the observation optics, the method becomes somewhat cumbersome by the need of complementing EM data.

Speciation

Cyclosporin induced phosphate inclusions in renal tissue: Cyclosporin is an immuno-suppressor which has proven its value in controlling the rejection of organ transplants. Its nephrotoxicity, however, promoted an extensive investigation of its effects. While minimal immuno-suppressive doses appear to be relatively non-toxic, high doses produce renal injury by the formation of micro-calcifications or metastatic calcifications. To clarify the mechanism of the cyclosporin nephrotoxicity, rats were treated with cyclosporin for 8 to 21 days with 12.5 to 50 mg$\cdot$kg^{-1} (Verbueken *et al.*, 1992). The kidney tissue was fixed and Ca was localised with the Von Kossa method. In rats which received 12.5 mg kg^{-1} cyclosporin for 21 days, the Von Kossa positive material was primarily seen in the tubular lumen from the outer medulla. In the periodic acid schiff (PAS)-stained rat kidney after this treatment, the calcifications were clearly observed with the light microscope as intraluminal concentric laminations. The calcific deposits were analyzed by TOF LMMS. Figure 7 shows the typical positive (**A**) and negative (**B**) mass spectra from a single

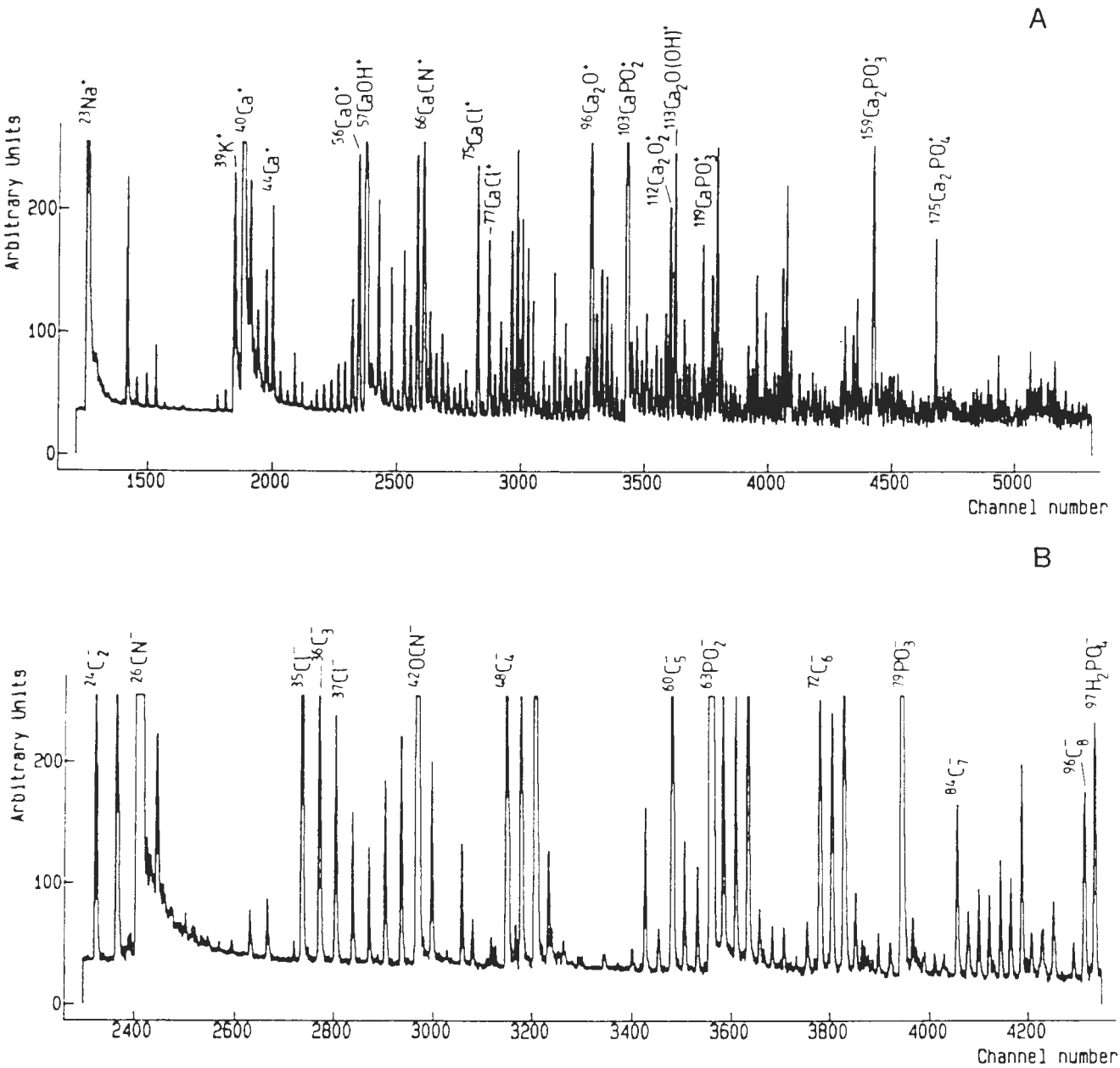

Figure 9. Corresponding (**A**) positive and (**B**) negative mass spectra of the spheroliths. The presence of calcium phosphate is based on the intense signals from at m/z 63 and 79, due to PO_2^- and PO_3^-, and at m/z 97, which can be partly attributed to $H_2PO_4^-$. In the positive mode, prominent peaks are observed for Ca^+, $CaO{\cdot}Ca^+$, $CaPO_3{\cdot}Ca^+$ and $CaPO_3{\cdot}CaO^+$ (with permission from Vandeputte *et al.*, 1989).

microlith. The data identify calcium phosphate as the main component. This is based on the prominent anions at m/z 63 and 79, due to PO_2^- and PO_3^-, and in the positive mode, the Ca^+ ions at m/z 40 accompanied by the cluster ions at m/z 103 and 159. The latter signal especially deserves attention. The ions at m/z 159 refer to a major structural building block of $Ca_3(PO_4)_2$ and, in practice, can be used for positive identification of the analyte (Struyf *et al.*, 1994). Unlike AEM or other microprobe techniques, identification does not rely on relative element abundances but on the desorption and ionisation of intact analytes. Their fragmentation occurs according to specified routes. As a result, the LMMS attains a higher information level than the cytochemical approach. The Von Kossa precipitation technique yields the detection of all available Ca, while LMMS specifies the molecule in which this calcium occurs. Note that the dimensions of the microliths range from 5 to 50 μm.

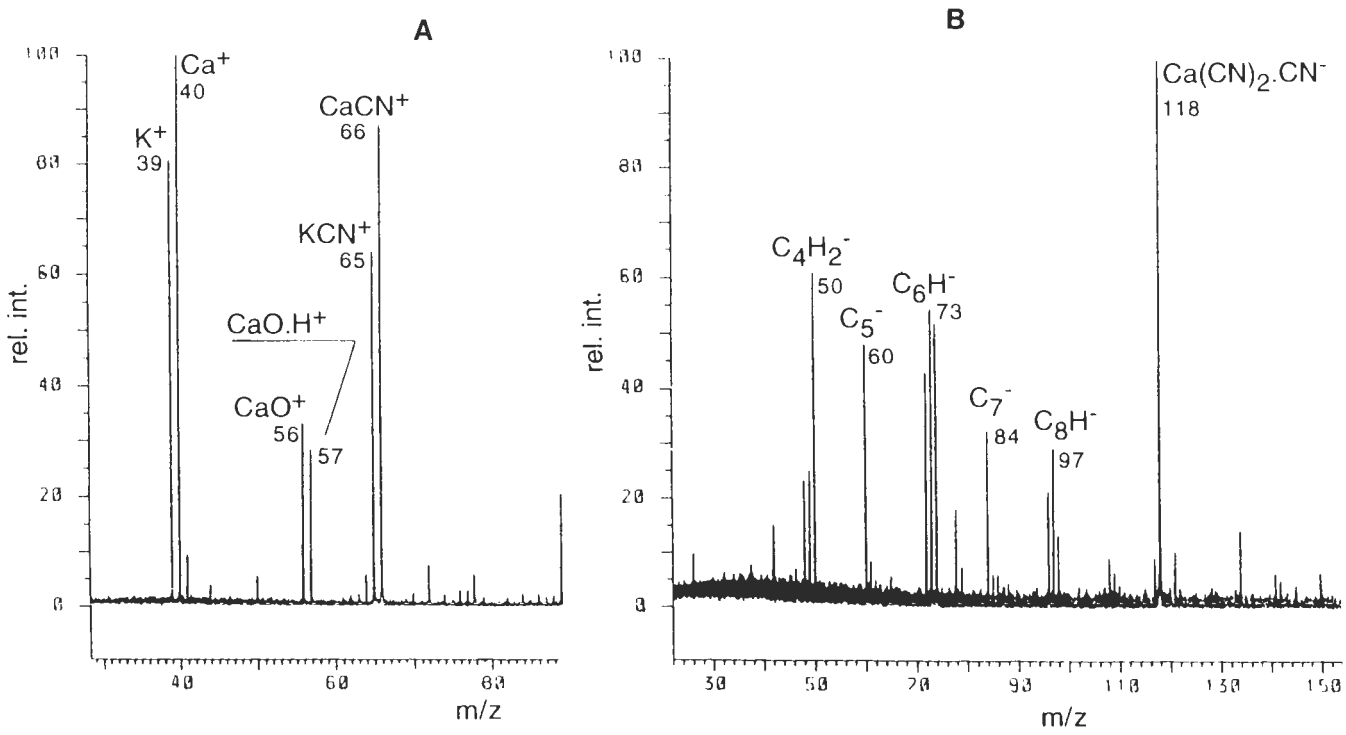

Figure 10. (**A**) Positive and (**B**) negative ion spectra of human vein grafts analyzed with FT LMMS. Calcium is detected in the positive mode at m/z = 40, and in the negative mode, the peak at m/z = 118 originates from $Ca(CN)_2 \cdot CN^-$.

This facilitates the identification in transmission TOF LMMS of which the spatial resolution is 1-2 μm under routine conditions. Micro-crystals in tissues also imply high analyte concentrations within the analyzed microvolume.

Spheroliths in primary atypical band keratopathy: The clinical picture from an elderly patient with a superficial corneal degeneration was a horizontal oval opacity in the lower central part of the cornea. The patient was treated by superficial keratectomy whereby the epithelium was removed and the underlying hazy Bowman's membrane was stripped. EM on the biopsy fragments showed numerous granules with a translucent centre and a dense periphery (Vandeputte *et al.*, 1989). TOF LMMS was used to verify the composition of these inclusions. The granules have an approximate diameter of 2 μm. Figure 8 shows the transmission electron micrographs of the Bowman's membrane of the patient before (**A**) and after (**B**) analysis. Figure 9 shows the positive (**A**) and negative (**B**) mass spectra of the spheroliths. The presence of calcium phosphate is based as in the previous case on the intense signals from PO_2^-, PO_3^- and from $H_2PO_4^-$ at m/z 97 in Figure 9B. In the positive mode (Fig. 9A), prominent peaks are observed for Ca^+, $CaO \cdot Ca^+$, $Ca_2PO_3^+$ and $CaO \cdot CaPO_3^+$. According to the systematics of LMMS speciation, the combination of these ions points to calcium phosphate. As opposed to the previous example, strong signals from the biological matrix also occur. Especially in the negative ion mass spectra, the total ion current is primarily carried by carbon clusters from the destruction of organic molecules. The relative concentration of the calcium phosphate in the analyzed microvolume is much lower than in the previous example. The straightforward speciation by LMMS becomes more difficult but remains feasible when the compound is more homogeneously distributed within a matrix.

Calcium deposition in transplanted human vein grafts: In a previous study, apoptotic cell death in the thickened intima of sub-occluded human saphenous vein grafts was demonstrated (Kockx *et al.*, 1994). This cell death was associated with luminal foam cell accumulation. Within the region of cell loss, calcium deposition was demonstrated by alizarin-red staining.

In order to specify the nature of the calcium deposits, FT LMMS was used.

Figure 10A shows the positive ion spectrum of a human vein graft. Although the base peak is due to K^+ at m/z 39, the peak intensity at m/z 40 reflects the high local Ca^+ level, consistent with the alizarin red staining procedure. The prominent peaks at m/z 57, 65 and 66 refer to $CaO \cdot H^+$, KCN^+ and $CaCN^+$ respectively. With respect to the speciation of the calcium compound, distinction must be made between for instance free or

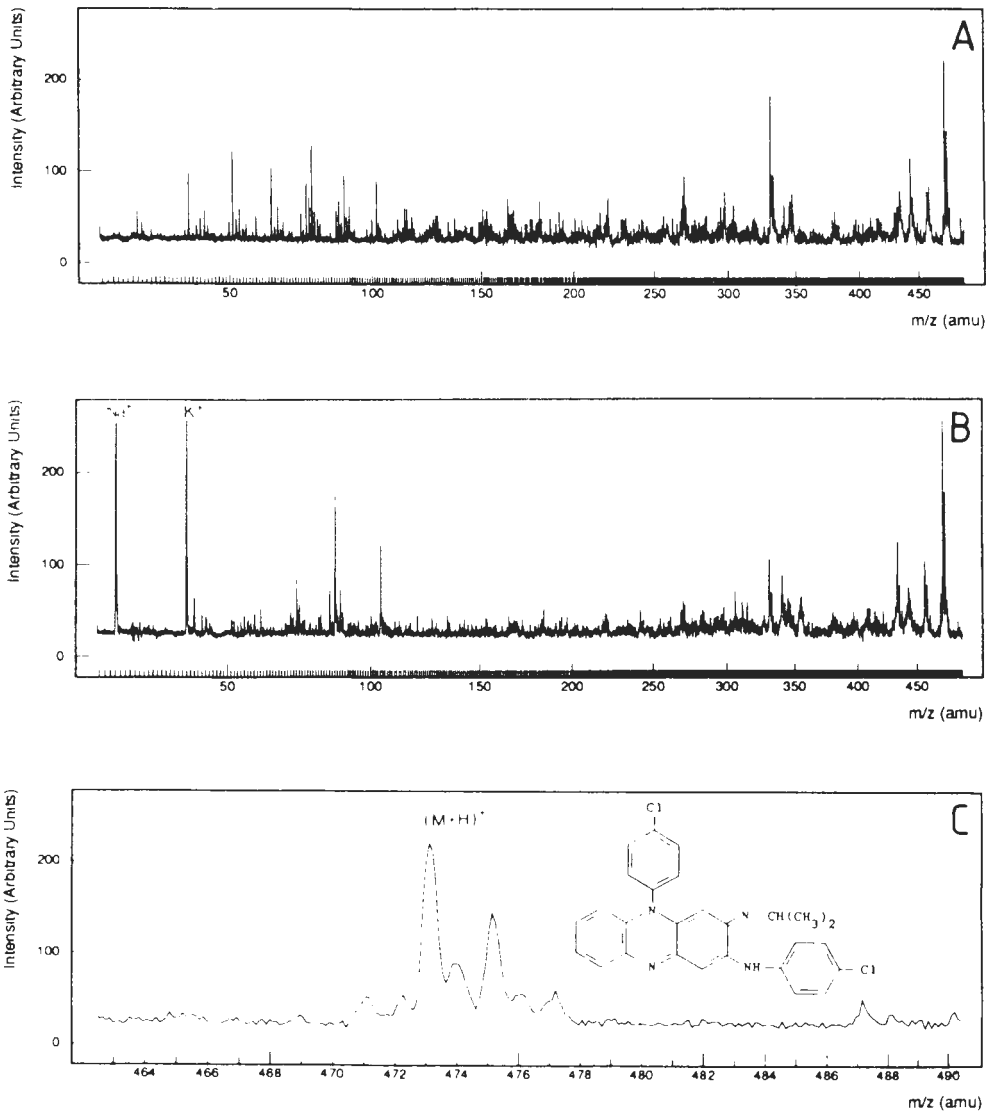

Figure 11. Comparison between the positive TOF LMMS results recorded from the crystals in the tissue (**A**) and (**B**), and the Clofazimine pure powder (**C**). The molecular weight is readily deduced from the $[M+H]^+$ ions at m/z 473 (**C**) (with permission from Vandeputte *et al.*, 1993).

bound Ca^{2+} and oxy-salts on the basis of the negative ion mass spectra (Struyf *et al.*, 1994). The main anions detected (Fig. 10B) constitute a typical distribution of $C_nH_m^-$(n = 4, 5, ..., m = 0, 1, 2, ...) ions, while the base peak is due to $Ca(CN)_2{\cdot}CN^-$. Note the absence of signals from common oxy-salt residues. Specifically, phosphate salts would yield intense signals at m/z 63 (PO_2^-) and 79 (PO_3^-). As a result, the occurrence of free or bound Ca^{2+}, but not in the form of an oxy-salt, was deduced. In contradiction to the findings of Fitzpatrick *et al.* (1994) in coronary atherosclerotic plaques, the calcifications, which we found in saphenous vein grafts, were not hydroxyapatite.

Organic molecules

Clofazimine deposition in mouse spleen: Leprosy is caused by *Mycobacterium leprae*. These mycobacteria predominantly reside and multiply in the basal lamina of the Schwann cells of unmyelinated nerve fibres and cause peripheral neuropathy. The blood-brain barrier could prevent the anti-mycobacterial drugs from reaching their target. Therefore, it is not yet clear whether the anti-leprosy drug clofazimine can enter the Schwann cells in sufficient quantities.

The present study was motivated by an interest in the localisation of Clofazimine (Vandeputte *et al.*, 1993). Cryosections of spleen cells from a treated mouse showed brick-red crystals. Figure 11 shows a comparison between the positive TOF LMMS results recorded from the crystals in the tissue and the Clofazimine pure powder. The molecular weight is readily deduced from the $[M+H]^+$ ions at m/z 473 (Fig. 11C). A series of structural fragments is detected above m/z 300 onwards for both the reference and the tissue sample. Signals in the low m/z range have little diagnostic value. The mass spectral pattern from the crystal in the tissue closely resembles the one from the pure product above m/z 300. Clofazimine is indeed one of the major

constituents of the crystalline deposits found in the mouse spleen. The porosity of cryosections facilitates the analysis in TOF LMMS.

***In situ* analysis of a perylene quinone in lichens:** Lichens are organisms which result from the symbiosis of fungi and algae. In tropical countries, barks of trees are colonized by corticulous micro-lichens. In the present study, two families are of interest: the Graphidaceae and the Trypetheliaceae family because their fruiting bodies are often pigmented. Although the chemical compounds in these highly pigmented lichens have been determined by application of UV, infrared (IR), nuclear magnetic resonance (NMR) or mass spectrometry after isolation and purification, the distribution of these organic molecules *in situ* remained unknown. In order to obtain data with respect to the localization and distribution of the identified products within the tissues, both TOF and FT LMMS have been applied (Mathey *et al.*, 1987, 1989, 1994). The visibility of the sample is better in the transmission type observation system of TOF LAMMA 500, but preparation of sectioned samples is required. FT LMMS works in reflection and hence is better suited to investigate bio-organisms at the surface of different materials while the mass resolution and accuracy are superior to TOF LMMS.

Figure 12 represents the positive mass spectra recorded by FT LMMS directly from the corticulous micro-lichen at the surface of a tree (Mathey *et al.*, 1994). A piece of bark was introduced without further sample preparation. Depending on the local potassium concentration, different peak patterns occur. High alkali levels permit detection of intact molecules in their cationised form $[M+K]^+$ (Fig. 12B) These signals allow to deduce the molecular weight, but not yet the structural features. This information, however, is nicely provided by the numerous fragments recorded from spots with low K^+ levels (Fig. 12A). The mass accuracy on detection of the ions is high so that the elemental composition unambiguously determined. As a result, structural assignment of the daughter ions is straightforward (Mathey *et al.*, 1994) so that the pigment could be identified as isohypocrelline. Note that the mass resolution is much better than can be seen from the compressed plot. The application of FT LMMS allows to eliminate the usual step of high resolution mass spectrometry on the isolated substances. Furthermore, the *in situ* analysis permits to retain the link with the localisation for the identified molecules in the specific biological environment.

Conclusions

We have discussed the combined application of especially morphological EM, AEM, PIXE and LMMS to local analysis in biomedicine and biology. The methods, currently used in our laboratory, complement, refine and/or extend the chemical information gained from light microscopy and cytochemical methods. To provide guidance in matching the technique to be used with the information wanted, different information levels were defined, both morphological and chemical in nature.

Localisation of elements is considered as the first level application. EM based techniques are best suited for high grade morphological investigation, i.e., at the subcellular level down to 10 nm. Whenever the detection limits in X-ray analysis are adequate, direct quantification is feasible in the complex biological matrix. Nuclear microscopy, especially PIXE, provides better sensitivity, excellent quantification capabilities but the observation of the sample could be improved, at least in the version we used. The routine application of nuclear microscopy is limited by the complexity and cost of the instrumentation and its operation. Therefore, in our laboratory, LMMS is still appreciated for element localisation in selected applications, in spite of the lack of straightforward quantification capabilities. Although the morphological resolution remains at the 1-5 μm level, the main advantage of LMMS resides in the possibility to get higher level chemical information.

Identification of inorganic molecules by means of signals referring to structural entities creates a superior level of information. Both AEM and nuclear microscopy essentially provide relative element abundances, but do not specify which elements belong to the same molecule. In contrast, LMMS generates structural ions from (almost) intact inorganic compounds in the same way as conventional mass spectrometry does with organic molecules. As a result, direct speciation capabilities are offered. The earlier TOF LMMS instruments were limited, making interpretation of the mass spectra often cumbersome. To fully exploit the information contained in the ions, a high resolution mass spectrometer is needed. In this respect, the recent development of the FT LMMS instruments proved to be a major step forward in the application of the method.

The localisation of organic molecules by means of structural signals represents the ultimate level of information. Up to now, the currently used methods could only detect organic molecules by the aid of cytochemical reactions. This approach is indirect and it depends on the specificity of the reactions involved. In contrast, LMMS is the only technique capable of generating signals corresponding to intact molecules or to very specific fragments from organic compounds.

Acknowledgements

Luc Van Vaeck is indebted to the National Science Foundation Belgium (NFWO) as research associate. The authors thank F. Lakiere for the photography.

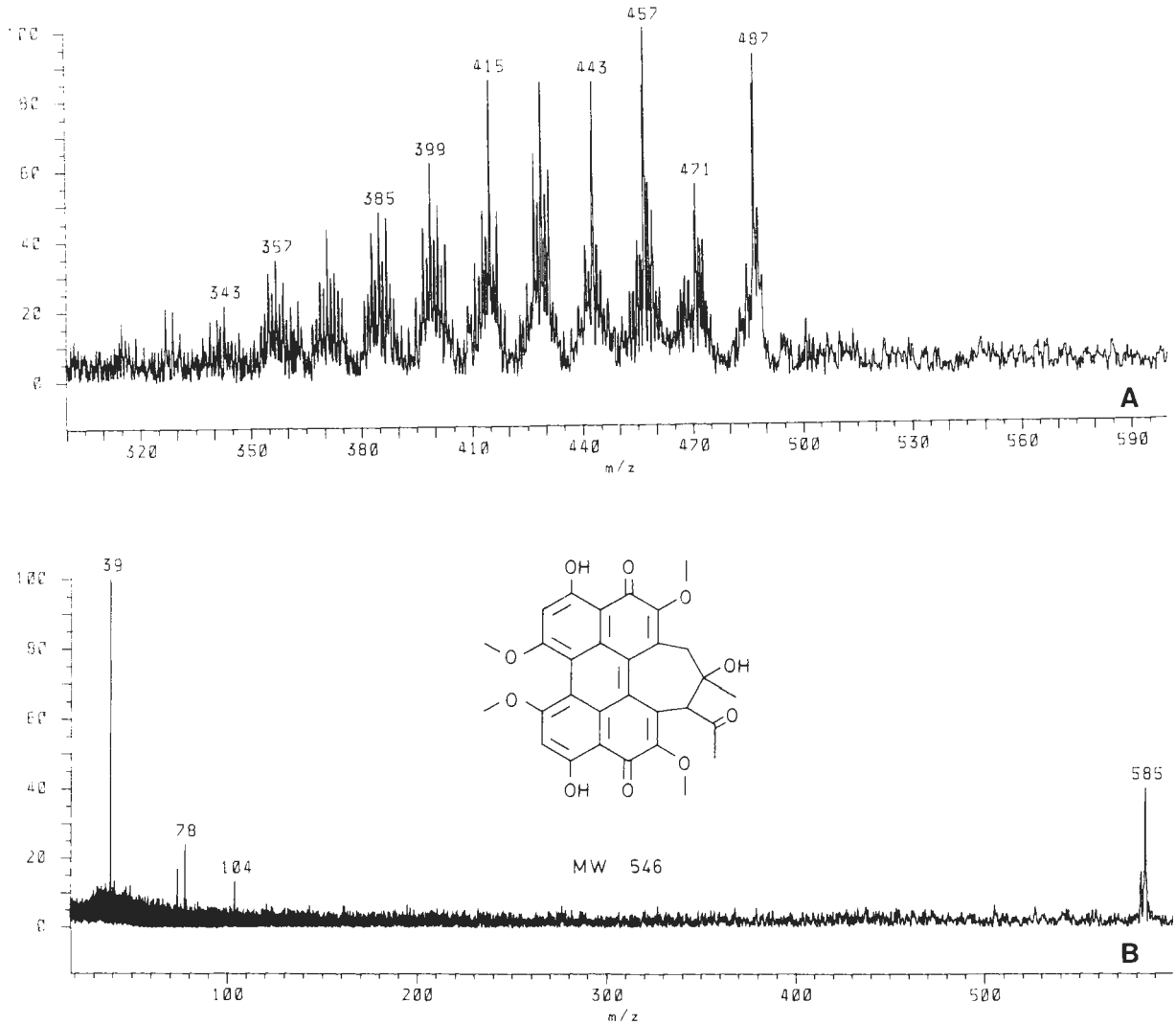

Figure 12. Positive ion mass spectra (of an isohypocrelline) recorded by FT LMMS directly from the corticolous micro-lichen at the surface of a tree in the presence of (**A**) low or (**B**) high alkali levels (with permission from Mathey *et al.*, 1994).

References

Baddeley AJ, Gundersen HJG, Cruz-Oriv LM (1986) Estimation of surface area from vertical sections. J Microsc **142**: 259-276.

Bakker A (1995) Mitochondrial contact sites: Calcium sensitive matrices for efficient enzyme activities. Doctoral Thesis. University of Antwerp. pp. 77-96.

Bakker A, De Bie M, Bernaert I, Ravingerova T, Ziegelhöffer A, Van Belle H, Jacob W (1993) Increased extracellular calcium concentrations in isolated rat heart: Effects on mitochondrial contact sites formation. Eur J Morphol **31**: 46-50.

Bakker A, Biermans W, Van Belle H, De Bie M, Bernaert I, Jacob W (1994a) Ultrastructural localisation of carnitine acetyltransferase activity in mitochondria of rat myocardium. Biochim Biophys Acta **1185**: 97-102.

Bakker A, Bernaert I, De Bie M, Ravingerova T, Ziegelhöffer A, Van Belle H, Jacob W (1994b) The effect of calcium on mitochondrial contact sites: A study on isolated rat hearts. Biochim Biophys Acta **1224**: 583-588.

Bakker A, Goossens F, De Bie M, Bernaert I, Van Belle H, Jacob W (1995a) The effect of ischaemia and reperfusion on mitochondrial contact sites in isolated rat hearts. Histol Histopathol **10**: 405-416.

Bakker A, De Nollin S, Van Vaeck L, Slezak J, Ravingerova T, Jacob W, Ruigrok TJC (1995b) Lidocaine does not prevent the calcium paradox in rat hearts: A laser microprobe mass analysis (lamma) study. Life

Sci **56**: 1601-1611.

Bara M, Guiet-Bara A, Moretto Ph (eds.) (1996) Nuclear microprobes in biology and medicine. Cell Molec Biol **42**: 1-134.

Bench GS, Legge GJF (1989) High resolution STIM. Nucl Instrum Meth **B40/41**: 655-658.

Benninghoven A, Rüdenauer FG, Werner HW (1987) Secondary Ion Mass Spectrometry. Chemical Analysis Series, Vol. 86. John Wiley and Sons, New YorK. pp. 329-663.

Biermans W, Bakker A, Jacob W (1990) Contact sites between inner and outer mitochondrial membrane: A dynamic compartment for creatine kinase activity. Biochim Biophys Acta **1018**: 225-228.

Breese MBH, Landsberg JP, King PJC, Grime GW, Watt F (1992) Applications of scanning transmission ion microscopy. Nucl Instrum Meth **B64**: 505-511.

Brenna JT (1989) Laser microprobe Fourier transform ion cyclotron resonance mass spectrometry: Instrumentation and results of polymer studies. In: Microbeam Analysis 1989. San Francisco Press, San Francisco. pp. 306-310.

Brenna JT (1991) Ultraviolet laser microprobe Fourier transform ion cyclotron resonance of organic and polymer surfaces. In: FT-ICR/MS Analytical Applications of Fourier Transform Ion Cyclotron Resonance Mass Spectrometry. Asamoto B (ed.). VCH Publishers, New York. pp. 187-213.

Brenna JT, Creasy WR (1988) Laser microprobe Fourier transform ion cyclotron mass spectrometry. In: Microbeam Analysis 1988. San Francisco Press, San Francisco. pp. 377-378.

Brenna JT, Creasy WR, McBain W, Soria C (1988) Nd:YAG laser microprobe system for Fourier-transform ion cyclotron resonance mass spectrometry. Rev Sci Instrum **59**: 873-879.

Burns-Belhorn MS, File DM (1979) Secondary ion mass spectrometry (SIMS) of standards for analysis of soft biological tissue. Anal Biochem **92**: 213-221.

De Nollin S, Jacob W, Van Vaeck L, Berger Y, Cautreels W, Remandet B, Vic P (1986) Subcellular localisation of a drug by two independent methods: Laser microprobe mass analysis and autoradiography. In: Proc. Third International Laser Microprobe Mass Spectrometry Workshop. Adams F, Van Vaeck L (eds.). Univ. Antwerp, Belgium. pp. 53-61.

Dingle T, Griffiths BW, Ruckman JC (1981) LIMA - A laser induced ion mass analyser. Vacuum **31**: 571-577.

Dingle T, Griffiths BW, Ruckman JC, Evans CA Jr (1982) The performance of a laser induced ion mass analyzer system for bulk samples. In: Microbeam Analysis 1982. San Francisco Press, San Francisco. pp. 365-368.

Edelman L (1994) Optimal freeze drying of cryosections and bulk specimens for X-ray microanalysis. Scanning Microsc Suppl **8**: 67-81.

Egerton RF (1986) Electron Energy-Loss Spectroscopy in the Electron Microscope. Plenum Press, New York. pp. 129-287.

Eeckhaoudt S (1994) Morphological and micro-analytical study of gills of fish exposed to aluminium at low pH. Doctoral Thesis, University of Antwerp. p. 5.

Eeckhaoudt S, Van Vaeck L, Gijbels R, Van Grieken R (1994) Laser microprobe mass spectrometry in biology and biomedicine. Scanning Microsc Suppl 8: 335-258.

Fitzpatrick LA, Severson A, Edwards WD, Ingram RT (1994) Diffuse calcification in human coronary arteries. J Clin Invest **94**: 1597-1604.

Forslind B, Emilson A (1992) Quantitative and computer assisted electron microscopic and microprobe studies in dermatology. Scanning Microsc **6**: 1155-1162.

Fragu P, Clerc J, Briancon C, Fourré C, Jeusset J, Halpern S (1994) Recent development in medical applications of SIMS microscopy. Micron **25**: 361-370.

Ghaderi S (1988) Applications of laser microprobe using Fourier transform mass spectrometry. In: Proc. 36th ASMS Conference on Mass Spectrometry and Allied Topics. Int Soc Mass Spectrometry, East Lansing, MI. pp. 1126-1127.

Glauert AM (1974) Fixation, Dehydration and Embedding of Biological Specimens. In: Practical Methods in Electron Microscopy, Vol 3. North-Holland Publ. Co., Amsterdam. pp. 1-176.

Grime GW, Dawson M, Marsh M, McArthur IC, Watt F (1991) The Oxford submicron nuclear microscopy facility. Nucl Instr Meth **B54**: 52-63.

Guest WH (1984) Recent developments of laser microprobe mass analysers, LAMMA 500 and 1000. Int J Mass Spectrom Ion Processes **60**: 189-199.

Hackenbrock CR (1968) Chemical and physical fixation of isolated mitochondria in low-energy and high-energy states. Proc Natl Acad Sci USA **61**: 598-605.

Heinen HJ, Meier S, Vogt H, Wechsung R (1983) LAMMA 1000, a new laser microprobe mass analyser for bulk samples. Int J Mass Spectrom Ion Phys **47**: 19-22.

Hillenkamp F, Unsöld E, Kaufmann R, Nitsche R (1975) A high-sensitivity laser microprobe mass analyser. Appl Phys **8**: 341-348.

Hillenkamp F, Feigl P, Schueler B (1982) Laser micro mass analysis of bulk surfaces. Microbeam Analysis 1982. San Francisco Press, San Francisco. pp. 359-364.

Holliman CL, Rempel DL, Gross ML (1994) Detection of high mass-to-charge ions by Fourier transform mass spectrometry. Mass Spectrom Rev **13**: 105-132.

Holm R, Holtkamp D (1989) LAMMS: applications in material science. In: Microbeam Analysis 1989. San

Francisco Press, San Francisco. pp. 325-329.

Housden J, Hutt KW, Wallach ER (1989) The question of ion yield in LAMMS. In: Microbeam Analysis 1989. San Francisco Press, San Francisco. pp. 269-272.

Jacob WA, De Nollin S, Hertsens RC, De Smet M (1984) Subcellular determination of trace amounts of Ca^{++}-ions in biological tissue. J Trace Microprobe Techn **2**: 161-184.

Jacob W, Biermans W, Bakker A (1992) Mitochondrial contact sites: A dynamic compartment for creatine kinase activity. In: Guanidino Compounds in Biology and Medicine. De Deyn PP, Marescau B, Stalon V (eds.). John Libbey & Co., London, UK. pp. 165-174.

Kaufmann R, Hillenkamp F, Wechsung R, Heinen HJ, Schürmann M (1979) Laser microprobe mass analysis: Achievements and aspects. Scanning Electron Microsc **1979**; II: 279-290.

Kaufmann R (1982) Laser microprobe mass analysis (LAMMA), current state of the art with special emphasis on bio-medical applications. In: Microbeam Analysis 1982. San Francisco Press, San Francisco. pp. 341-358.

Kaufmann R, Rechmann P, Tourmann JL, Schnatz H (1989) LAMMS in biomedical research: Achievements, shortcomings, promises. In: Microbeam Analysis 1989. San Francisco Press, San Francisco. pp. 35-42.

Kaufmann R, Spengler B (1992a) Laser microprobe mass spectrometry: A trend analysis. In: Proc. 50th Ann. Meet. Electron Microscopy Society of America. San Francisco Press, San Francisco. pp. 1558-1559.

Kaufmann R, Spengler B (1992b) Laser (micro)-probe mass spectrometry (LAMMS): Achievements and future trends in life sciences. In: Proc. 50th Ann. Meet. Electron Microscopy Society of America. San Francisco Press, San Francisco. pp. 1598-1599.

Knoll G, Brdiczka D (1983) Changes in freeze-fractured mitochondrial membranes correlated to their energetic state. Dynamic interactions of the boundary membranes. Biochim Biophys Acta **733**: 102-110.

Kockx MM, Cambier BA, Bortier HE, De Meyer GR, Declercq SC, Van Cauwelaert PA, Bultinck J (1994) Foam cell replication and smooth muscle cell apoptosis in human saphenous vein grafts. Histopathol **25**: 365-371.

Krier G, Masselon C, Muller JF, Nelieu S, Einhorn J (1994) Laser-desorption Fourier-transform mass spectrometry of triazines adsorbed on solid-phase Extraction Membranes. Rapid Commun Mass Spectrom **8**: 22-25.

Lorimer GW (1984) Quantitative X-ray microanalysis of thin specimens. In: Quantitative Electron Microscopy. Chapman JN, Craven AJ (eds.). Scottish Universities Summer School in Physics, Edinburgh, Scotland. pp. 305-339.

Malmqvist KG (1986) Proton microprobe analysis in biology. Scanning Electron Microsc **1986**; III: 821-845.

Mamyrin BA, Karataev VI, Shmikk DV, Zagulin VA (1973) The mass-reflectron, a new nonmagnetic time-of-flight mass spectrometer with high resolution. Sov Phys-JETP **37**: 45-48.

Marshall AG, Verdun FR (1990) Fourier transforms in NMR, optical and MS: A user's handbook. Elsevier, New York. pp. 225-278.

Mathey A, Van Vaeck L, Steglich W (1987) Investigation of semi-thin cryosections of lichens by laser microprobe mass spectrometry. Anal Chim Acta **195**: 89-96.

Mathey A, Van Vaeck L, Ricci P (1989) *In situ* analysis of carnation phytoalexines by laser microprobe mass spectrometry. In: Microbeam Analysis 1989. San Francisco Press, San Francisco. pp. 350-352.

Mathey A, Van Roy W, Van Vaeck L, Eckhardt G, Steglich W (1994) *In situ* analysis of a new perylene quinone in lichens by Fourier-transform laser microprobe mass spectrometry with external source. Rapid Comm Mass Spectrom **8**: 46-52.

Mauney T, Adams F (1984) Ion kinetic energy measurements on laser-induced plasmas in Laser Microprobe Mass Analysis (LAMMA). Part I. Methodology. Int J Mass Spectrom Ion Processes **59**: 103-119.

Mauney T (1985) Quantitative laser microprobe mass spectrometry: potential and constraints. In: Microbeam Analysis 1985. San Francisco Press, San Francisco. pp. 299-304.

Michiels E, Mauney T, Adams F, Gijbels R (1984) Ion kinetic energy measurements on laser-induced plasmas in laser microprobe mass analysis (LAMMA) Part 2. Titanium dioxide. Int J Mass Spectrom Ion Processes **61**: 231-246.

Muller JF, Krier G, Verdun F, Muller D (1985a) Laser ionization and laser desorption with tunable wavelength. Recent developments and perspectives. In: Advances in Mass Spectrometry 1985. Todd JFJ (ed.). John Wiley & Sons, Chichester, UK. pp. 1593-1594.

Muller JF, Krier G, Verdun F, Lamboule M, Muller D (1985b) Ionization of organic crystals with a tunable dye laser connected to a LAMMA instrument. Int J Mass Spectrom Ion Processes **64**: 127-138.

Odom RW, Schueler B (1990) Laser microprobe mass spectrometry: Ion and neutral analysis. In: Lasers and Mass Spectrometry. Lubman DM (ed.). Oxford University Press, New York. pp. 103-137.

Pelletier M, Krier G, Muller JF, Weil D, Johnston M (1988) Laser microprobe Fourier transform mass spectrometry. Rapid Commun Mass Spectrom **2**: 146-150.

Reimer L (1989). Transmission Electron Microscopy. Springer Verlag, Berlin. p. 5 and 14.

Ruckman JC, Davey AR, Clarke NS (1984) Laser-

induced ion mass analysis: A novel technique for solid-state examination. Vacuum **34**: 911-924.

Schueler B, Odom RW (1987) Nonresonant multiphoton ionization of the neutrals ablated in laser microprobe mass spectrometry analysis of GaAs and $Hg_{0.78}Cd_{0.22}Te$. J Appl Phys **61**: 4652-4661.

Southon MJ, Witt MC, Harris A, Wallach ER, Myatt J (1984) Laser-microprobe mass analysis of surface layers and bulk solids. Vacuum **34**: 903-909.

Struyf H, Van Roy W, Van Vaeck L, Van Grieken R, Caravatti P (1994) The Fourier-transform laser microprobe mass spectrometer with external ion source as a tool for inorganic microanalysis. Rapid Commun Mass Spectrom **8**: 32-39.

Szokefalvi-Nagy Z (1994) Applications of PIXE in the life sciences. Biol Trace Element Res **43-45**: 73-78.

Vandeputte DF, Van Grieken RE, Foets BJJ, Misotten L (1989) Characterization of spherolyths present in primary atypical bandkeratopathy using laser microprobe mass analysis. Biomed Environ Mass Spectrom **18**: 753-756.

Vandeputte D, Jacob W, Van Grieken R, Boddingius J (1993) Study of intracellular deposition of antileprosy drug Clofazimine in mouse spleen using Laser Microprobe Mass Analysis. Biol Mass Spectrom **22**: 221-225.

Van Roy W, Struyf H, Van Vaeck L, Gijbels R, Caravatti P (1994) A Fourier transform laser microprobe mass spectrometer with external ion source for organic and inorganic surface and micro-analysis. In: Secondary Ion Mass Spectrometry SIMS IX. Benninghoven A, Nihei Y, Shimigu R, Werner HW (eds.). John Wiley & Sons, Chichester, UK. pp. 463-467.

Van Vaeck L, Claereboudt J, Van Espen P, Adams F, Gijbels R, Cautreels W (1985) On the use of LAMMA for microprobing of organic compounds in biological samples. In: Advances in Mass Spectrometry 1985. Todd JFJ (ed.). John Wiley & Sons, Chichester, UK. pp. 957-958.

Van Vaeck L, Van Espen P, Jacob W, Gijbels R, Cautreels W (1988) In depth limitation of the LAMMA 500 for the *in situ* localisation of organic compounds in biological embedded tissue samples. Biomed Environ Mass Spectrom **16**: 113-119.

Van Vaeck L, Van Roy W, Gijbels R, Adams F (1993a) Lasers in mass spectrometry: Organic and inorganic instrumentation. In: Laser Ionization Mass Analysis. Vertes A, Gijbels R, Adams F (eds.). Chemical Analysis Series. Vol. 124. John Wiley and Sons Inc., New York. pp. 7-126.

Van Vaeck L, Van Roy W, Struyf H, Adams F, Caravatti P (1993b) Development of a new Fourier transform laser microprobe mass spectrometer with external ion source. Rapid Commun Mass Spectrom **7**: 323-331.

Van Vaeck L, Struyf H, Van Roy W, Adams F (1994a) Organic and inorganic analysis with lasers microprobe mass spectrometry. Part 1: Instrumentation and methodology. Mass Spectrom Rev **13**: 189-208.

Van Vaeck L, Struyf H, Van Roy W, Adams F (1994b) Organic and inorganic analysis with lasers microprobe mass spectrometry. Part 2: Applications. Mass Spectrom Rev **13**: 209-232.

Verbueken AH, Bruynseels FJ, Van Grieken RE (1985) Laser microprobe mass analysis: A review of applications in the life sciences. Biomed Mass Spectrom **12**: 438-463.

Verbueken AH, Bruynseels FJ, Van Grieken R, Adams F (1988) Laser microprobe mass spectrometry. In: Inorganic Mass Spectrometry. Adams F, Gijbels R, Van Grieken R (eds.). John Wiley & Sons, New York. pp. 173-254.

Verbueken AH, Van Grieken R, Verpooten GA, De Broe ME, Wedden RP (1992) Laser microprobe mass spectrometric identification of cyclosporin-induced intrarenal microliths in rat. Biol Mass Spectrometry **21**: 590-596.

Verdun FR, Krier G, Muller JF (1987) Increased sensitivity in laser microprobe mass analysis by using resonant two-photon ionization processes. Anal Chem **59**: 1383-1387.

Vogt H, Heinen HJ, Meier S, Wechsung R (1981) LAMMA 500: Principle and technical description of the instrument. Fresenius' Z Anal Chem **308**: 195-200.

Wallimann T (1994) Dissecting the role of creatine kinase. Curr Biol **1**: 42-46.

Watt F, Grime GW (1988) Elemental mapping of biological samples using a scanning proton microprobe. Nucl Instr Meth **B30**: 356-366.

Watt F, Grime GW, Brook AJ, Gadd GM, Perry CC, Pearce RB, Turnau K, Watkinson SC (1990) Nuclear microscopy of biological specimens. Nucl Instr Meth **B54**: 123-143.

Wechsung R, Hillenkamp F, Kaufmann R, Nitsche R, Vogt H (1978) LAMMA - A new laser microprobe mass analyzer. Scanning Electron Microsc **1978**; I: 611-620.

Zimmerman ANE, Hülsmann WC (1966) Paradoxal influence of calcium ions on the permeability of the cell membranes of the isolated rat heart. Nature **211**: 646-647.

Discussion with Reviewers

Reviewer I: The FT LMMS technique looks like promising a second generation and much improved LMMS. However, in view of biomedical applications, I would like to have comments on a number of aspects. (1) In my experience, the transmission geometry is much better

for biological samples. Do you think it ever will be possible in FT LMMS? (2) Can the lateral resolution be improved? (3) Will mapping be possible?

Authors: (1) The reflection geometry of the FT LMMS instruments issues from the applications in the material sciences at which this technique is aimed. With regard to our instrument, conversion to the transmission mode would imply a major change of the ion source assembly, but is feasible. Up to now, there is no real evidence for a possibly better ion yield in transmission. Therefore, illumination of the sample in transmission would already alleviate the problem of tissue analysis in reflection. This is much simpler to implement, and planned in our laboratory for the very near future.

(2) The diffraction limited spot of 0.5 μm could be achieved in FT LMMS, but would complicate the construction of the ion source optics. Because only ions within a limited energy range (about 1 eV) can be trapped in the cell, the potentials in the immediate vicinity of the sample become more critical than in TOF LMMS. As a result, the external ion source in FT LMMS requires a more complicated electrode geometry around the sample. However, one has also to realise that the irradiated area directly determines the sample consumption and the number of ions generated upon each single laser interaction. Up to now, the sensitivity of FT LMMS (absolute number of ions needed for detection) is about one order of magnitude lower than that in TOF LMMS. The larger spot size compensates this so that both instruments can deal with the same local concentrations in the surface layer.

(3) Motorisation of the micromanipulators is easy to achieve while data acquisition can be fully automated. This would provide mapping for perfectly flat samples, since the specimen surface must not be repositioned in the waist of the laser. Most samples are not flat within a μm and the spot size is extremely important to obtain reproducible and reliable results. Hence, mapping would practically imply that an imaging system for automated refocusing would be incorporated. Furthermore, proper data processing programs must be developed to handle the massive amount of data. The problem is aggravated in comparison to TOF LMMS because of the high mass resolution in FT LMMS. As a result, mapping becomes a major development.

Reviewer I: How can you compare FT to TOF LMMS in terms of complexity of operation, running cost, time per analysis?

Authors: The progress in mass resolution and mass accuracy made in FT LMMS is several orders of magnitude better than in TOF LMMS while the sensitivity does not decrease proportionally. The price to be paid is indeed the complexity of instrumental tuning and spectrum acquisition. FT LMMS needs skilled operators while TOF LMMS is better suited to multi-user operation. The typical analysis time per sample in FT LMMS is 3 to 5 times longer than in TOF LMMS. However, TOF LMMS usually needs comparison with reference samples while the high mass accuracy and resolution ion FT LMMS enables us to eliminate this step. The running cost of FT LMMS is comparable to that of TOF LMMS apart from the liquid gases for the superconducting magnet.

Reviewer I: In practice, do you really need the very high mass resolution so that single ion monitoring is practically required as opposed to panoramic registration?

Authors: The mass resolution at low m/z exceeds what one really needs to separate the isobaric interferences. A mass resolution in the order of 10,000 to 20,000 would be sufficient for most practical applications, on the condition that the mass accuracy remains within 1 ppm. However, by the principle of FTMS, mass resolution parallels sensitivity because in a first approximation, the same physical phenomenons are responsible for the loss of sensitivity and loss of resolution. Alternative mass analyzers for high mass resolution would be a double focusing magnetic instrument, but then the detection limits for short ionisation pulses would be lower. The problem of single ion monitoring versus panoramic registration is a technical one. At this moment, a home built multiple ion monitoring system is operational so that several selected ions can be detected upon each shot. Full panoramic registration involves a very large frequency bandwidth so that compromises must be made between sampling frequency and observation period, dictated by the memory capacity of the transient recorder.

Reviewer I: What about the organic high molecular weight compounds? Will measuring these become possible in the (near) future?

Authors: The matrix assisted laser desorption ionisation (MALDI) allows the mass spectrometric characterisation of high molecular weight organic compounds up to several hundreds of kDa. Up to now, only TOF mass analyzers can detect such high m/z, FTMS is limited to about m/z 15 000. One has to realise however that the sample must be dissolved in a matrix solution. This approach seems not yet compatible with localisation in a tissue. The irradiation of the sample by the laser only deliberates organics up to 1-2 kDa, partly as ions, which can be detected as such, partly as neutrals. The latter ones will be detectable by the application of post-ionisation, that we planned to try in the very future. Another aspect to consider is the local concentration. As opposed to elemental ions, organic molecules produce frag-

ments and hence, distribute the total ion current over numerous peaks. The detection limit for each signal individually rises proportionally. Organic molecules require a more critical tuning of the applied power density while elemental ions cannot undergo fragmentation at high irradiances. Finally, the thickness of the surface layer from which organic ions can be generated is certainly lower than for inorganic ions. As a result, it is assumed that the local concentration of organic compounds in the upper 10 nm of the evaporated volume of solid must be in the percent range.

B. Forslind: A comparison of LMMS with PIXE/X-ray microanalysis should include analysis of specified elements in stoichiometric amounts in a standard organic matrix such as used for calibration at particle probe analysis. Only then can the biological feasibility of LMMS be evaluated as compared to other techniques.
Authors: We agree that this is a key-problem in LMMS. We have demonstrated that both TOF and FT LMMS attain an acceptable degree of reproducibility, i.e., within 10% under controlled conditions on pure products as well as on selected mixtures (Van Vaeck and Gijbels, 1990; Van Vaeck *et al.* 1993c; Köllensperger *et al.*, 1996; Struyf *et al.*, 1996). However, several approaches were tried to prepare suitable standard materials, e.g., doping of resin sections, microcrystals with deposited layers to provide an internal standard, etc. The variability in signal detection was then assigned to local heterogeneities. Other techniques can only help to assess the quality of the standard on the condition that these methods are depending on the same compositional or physical influences. Furthermore, it is known that the micromorphology of the sample greatly influences the ion yield in LMMS (Musselman *et al.*, 1988). The same applies to the composition of the "matrix", i.e., the compounds accompanying the analyte of interest in the evaporated microvolume, as evidenced in an extreme way by the MALDI technique. The explanation is that the local energy regime in the sample region from where the ions actually issue depends on UV absorption, refraction and reflection of the sample in the specific spot. Standards for LMMS requires that these parameters can be kept comparable from spot-to-spot, which is not at all obvious in most sample preparation procedures. Furthermore, this addresses a fundamental problem. It is not yet sure if a given standard will be adequate to be used for biological material, given the heterogeneous nature of a tissue sample with respect to composition and "optical" interfaces.

G.M. Roomans: What about cryo versus embedding as sample preparation procedure?
Authors: This choice depends on the interaction between the chemists, who focus on the analytical aspects of their method, and the biologists, taking care of the sample preparation. From the chemist's point of view, cryo is preferred. Embedding inevitably involves the dilution of the local concentration of the tissue components as opposed to cryo-components, where the "inner space" is empty. Detection requires about 10^9 atoms or molecules in the upper 10 to 50 nm of the sample. This requirement is more easily met by cryo- than by embedded specimens. In particular, FT LMMS is also sensitive to the number of ions. The ions from the embedding medium do not give real information but increase the space charging in the cell and hence, degrade the detection limits.

However, from the biologist's point view, the situation can be a little be different. When it could be advantageous to use cryo-lyophilized material, this would require expensive apparatus (slam freezer or even high pressure freezer, cryo-ultramicrotome, cryotransfer to the microscope), which are not always available at all laboratories. Therefore, the classical embedding procedures are sometimes well worth to be optimised in function of a given problem. For instance, we have developed a method for Ca-precipitation using combined oxalate-pyroantimonate precipitation via cold perfusion (Jacob *et al.*, 1984). A drawback is that one cannot use EDS. Using this method, we could see minute changes in Ca-concentration (in the micromolar range) in mitochondria with different metabolic situations (Jacob *et al.*, 1990, 1994). This also holds for ischemia-reperfusion work. Of course, X-ray microanalysis would perhaps result in more quantitative results. But, using a standardised fixation and measuring method and the six significant LMMS levels, changes in the Ca concentration, even after fixation, is apparent. At least in physiological situations in the heart, it can be correlated with the number of contact sites, and thus becomes a morphological tool for the measurement of Ca content.

The dislike for stained sections in LMMS is primarily motivated by the common contaminants introduced by the procedure. If proper precautions are taken, staining can be helpful to facilitate the sample observation during chemical analysis. The mass resolution in FT LMMS practically eliminates interference problems, which can be an argument against staining in TOF LMMS.

Additional References

Jacob WA, Hertsens R, Van Bogaert A, De Smet M (1990) Mitochondrial matrix calcium ions regulate energy production in myocardium. A cytochemical study. In: Proc. XIIth International Congress of Electron Microscopy, Vol. 2. San Francisco Press, San Francisco. pp.

166-167.

Jacob WA, Bakker A, Hertsens RC, Biermans W (1994) Mitochondrial matrix granules: Their behaviour during changing metabolic situations and their relationship to contact sites between inner and outer mitochondrial membranes. Microsc Res Techn **27**: 307-318.

Köllensperger G, Poels K, Van Vaeck L, Struyf H, Van Roy W, Grasserbauer M (1996) Matrix assisted laser desorption ionisation of low molecular weight compounds by Fourier transform laser microprobe mass spectrometry with external source. Rapid Commun Mass Spectrom **10**: 538-550.

Musselman IH, Simons DS, Linton RW (1988) Effect of sample geometry on inter-element quantitation in laser microprobe mass spectrometry. In: Microbeam Analysis 1988. San Francisco Press, San Francisco. pp. 356-364.

Struyf H, Van Vaeck L, Van Grieken R (1996) Desorption-ionization of inorganic compounds in Fourier transform laser microprobe mass spectrometry with external ion source. Rapid Commun Mass Spectrom **10**: 551-561.

Van Vaeck L, Gijbels R (1990) Laser microprobe mass spectrometry: potential and limitations for inorganic and organic micro-analysis. Part 1. Techniques and inorganic applications. Fresenius' J Anal Chem **337**: 743-754.

Van Vaeck L, Van Roy W, Gijbels R, Adams F (1993c) Structural characterization of organic molecules by laser mass spectrometry. In: Laser Ionization Mass Analysis. Chemical Analysis Series. Vol. 124. Vertes A, Gijbels R, Adams F (eds.). John Wiley and Sons Inc., New York. pp. 177-319.